

# *Cenozoic evolution of the abrupt Colorado Plateau–Basin and Range boundary, northwest Arizona: A tale of three basins, immense lacustrine-evaporite deposits, and the nascent Colorado River*

**James E. Faulds\***

*Nevada Bureau of Mines and Geology, MS 178, University of Nevada, Reno, Nevada 89557, USA*

**Keith A. Howard\***

*U.S. Geological Survey, MS 973, Menlo Park, California 94025, USA*

**Ernest M. Duebendorfer\***

*Department of Geology, Northern Arizona University, Flagstaff, Arizona 86011, USA*

## ABSTRACT

In northwest Arizona, the relatively unextended Colorado Plateau gives way abruptly to the highly extended Colorado River extensional corridor within the Basin and Range province along a system of major west-dipping normal faults, including the Grand Wash fault zone and South Virgin–White Hills detachment fault. Large growth-fault basins developed in the hanging walls of these faults. Lowering of base level in the corridor facilitated development of the Colorado River and Grand Canyon. This trip explores stratigraphic constraints on the timing of deformation and paleogeographic evolution of the region. Highlights include growth-fault relations that constrain the timing of structural demarcation between the Colorado Plateau and Basin and Range, major fault zones, synextensional megabreccia deposits, non-marine carbonate and halite deposits that immediately predate arrival of the Colorado River, and a basalt flow interbedded with Colorado River sediments.

Structural and stratigraphic relations indicate that the current physiography of the Colorado Plateau–Basin and Range boundary in northwest Arizona began developing ca. 16 Ma, was essentially established by 13 Ma, and has changed little since ca. 8 Ma. The antiquity and abruptness of this boundary, as well as the stratigraphic record, suggest significant headward erosion into the high-standing plateau in middle Miocene time. Thick late Miocene evaporite and lacustrine deposits indicate that a long period of internal drainage followed the onset of extension. The widespread distribution of such deposits may signify, however, a large influx of surface waters and/or groundwater from the Colorado Plateau possibly from a precursor to the Colorado River. Stratigraphic relations bracket arrival of a through-flowing Colorado River between 5.6 and 4.4 Ma.

**Keywords:** Basin and Range, Colorado River, extension, paleogeography, Colorado Plateau

---

\*jfaulds@unr.edu; khoward@usgs.gov; ernie.d@nau.edu

Faulds, J.E., Howard, K.A., Duebendorfer, E.M., 2008, Cenozoic evolution of the abrupt Colorado Plateau–Basin and Range boundary, northwest Arizona: A tale of three basins, immense lacustrine-evaporite deposits, and the nascent Colorado River, *in* Duebendorfer, E.M., and Smith, E.I., eds., *Field Guide to Plutons, Volcanoes, Faults, Reefs, Dinosaurs, and Possible Glaciation in Selected Areas of Arizona, California, and Nevada: Geological Society of America Field Guide 11*, p. 119–151, doi: 10.1130/2008.fld011(06). For permission to copy, contact editing@geosociety.org. ©2008 The Geological Society of America. All rights reserved.

## INTRODUCTION

In northwest Arizona, the Colorado River crosses an unusually abrupt boundary between the Colorado Plateau and the Basin and Range province (Fig. 1). Essentially flat, relatively unextended strata on the high-standing Colorado Plateau give way to moderately to steeply tilted fault blocks in the Basin and Range province across a system of west-dipping normal faults that includes the Grand Wash fault zone (Lucchitta, 1966, 1979) and South Virgin–White Hills detachment fault (Fig. 2). Unlike other parts of the Colorado Plateau–Basin and Range boundary (e.g., southwest Utah and central Arizona), a broad transition zone is missing in northwest Arizona (Fig. 1). Instead, a 100-km-wide region of highly extended crust within the Basin and Range, referred to as the northern Colorado River extensional corridor (Faulds et al., 1990), directly borders the Colorado Plateau on the west. Within the footwall of the Grand Wash fault zone, the western edge of the Colorado Plateau is marked by

the imposing, west-facing fault-line escarpment of the Grand Wash Cliffs, which consist of subhorizontal Paleozoic strata rising  $\sim 1.3$  km above several east-tilted half grabens in the corridor, including the Grand Wash trough and the Hualapai basin. With respect to the base of the Tertiary section, structural relief across the Grand Wash fault zone commonly exceeds 5 km. Approximately 15–30 km west of the Grand Wash Cliffs, the gently west-dipping South Virgin–White Hills detachment fault dissects the corridor. The South Virgin–White Hills detachment fault is one of the most prominent structures in the northern part of the corridor, as it accommodated as much as 17 km of normal displacement and has many characteristics of classic detachment faults (Duebendorfer and Sharp, 1998; Brady et al., 2000). Thus, the transition between the essentially unextended Colorado Plateau to the highly attenuated Basin and Range occurs across a relatively narrow  $\sim 30$ -km-wide region in northwest Arizona.

It is noteworthy that the Colorado River flows transversely across this abrupt strain gradient, having excavated the Grand Canyon within the western part of the Colorado Plateau and traversing orthogonal to the structural grain within the Lake Mead region in the northern part of the extensional corridor (Figs. 2 and 3). The evolution of the Colorado River and Grand Canyon have long fascinated geoscientists, and many models have been proposed for its development (e.g., Powell, 1875, 1895; Blackwelder, 1934; Longwell, 1946; Hunt, 1969; Lucchitta, 1966, 1972, 1979, 1989; Young and Spamer, 2001). Recent work has greatly refined the evolution of the Colorado River, particularly the timing of inception for reaches downstream of the Grand Canyon (Spencer et al., 2001; Faulds et al., 2001b, 2002a; House et al., 2005; Dorsey et al., 2007), models for drainage development (Spencer and Pearthree, 2001; House et al., 2005), and rates of incision within the Grand Canyon (Fenton et al., 2001; Pederson and Karlstrom, 2001; Pederson et al., 2002). However, the relationships between major precursor events and development of the Grand Canyon and lower Colorado River have received less attention.

Clearly, the structural and topographic foundering of the Basin and Range province, particularly within the Colorado River extensional corridor, promoted excavation of at least the western part of the Grand Canyon within the high-standing Colorado Plateau. Understanding the spatial and temporal patterns of deformation within the extensional corridor is therefore critical for establishing a physiographic, structural, and temporal framework by which to assess the evolution of the Colorado River and associated drainage systems. On this field trip, we will evaluate the timing and nature of Cenozoic structural demarcation between the Colorado Plateau and the Basin and Range province in northwest Arizona (Fig. 3), as chronicled in the stratigraphy of major half grabens in the hanging walls of the Grand Wash and South Virgin–White Hills fault zones. A major goal of the trip is to further elucidate the relations between the stratigraphy and deformational history of these basins with the evolution of the Colorado River.

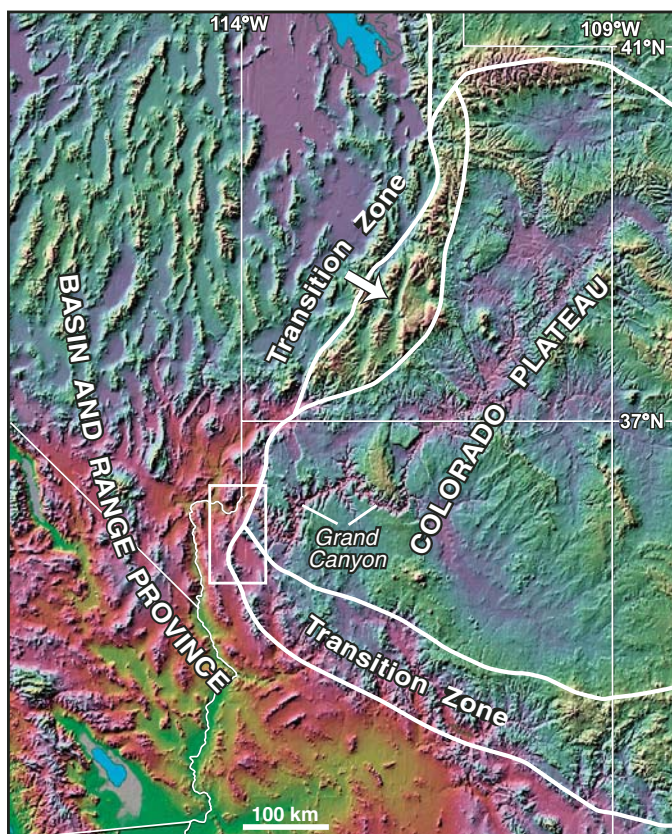


Figure 1. Digital elevation model showing the abrupt western margin of the Colorado Plateau. In contrast to broad transition zones throughout much of Utah and Arizona, the Colorado Plateau gives way abruptly westward to the Basin and Range province in the Lake Mead region of northwestern Arizona. Small white box encompasses the study area in the southern White Hills. The map projection is cylindrical and equidistant with the shape corrected for  $37.5^\circ$  north latitude. Lighting is from the northwest.



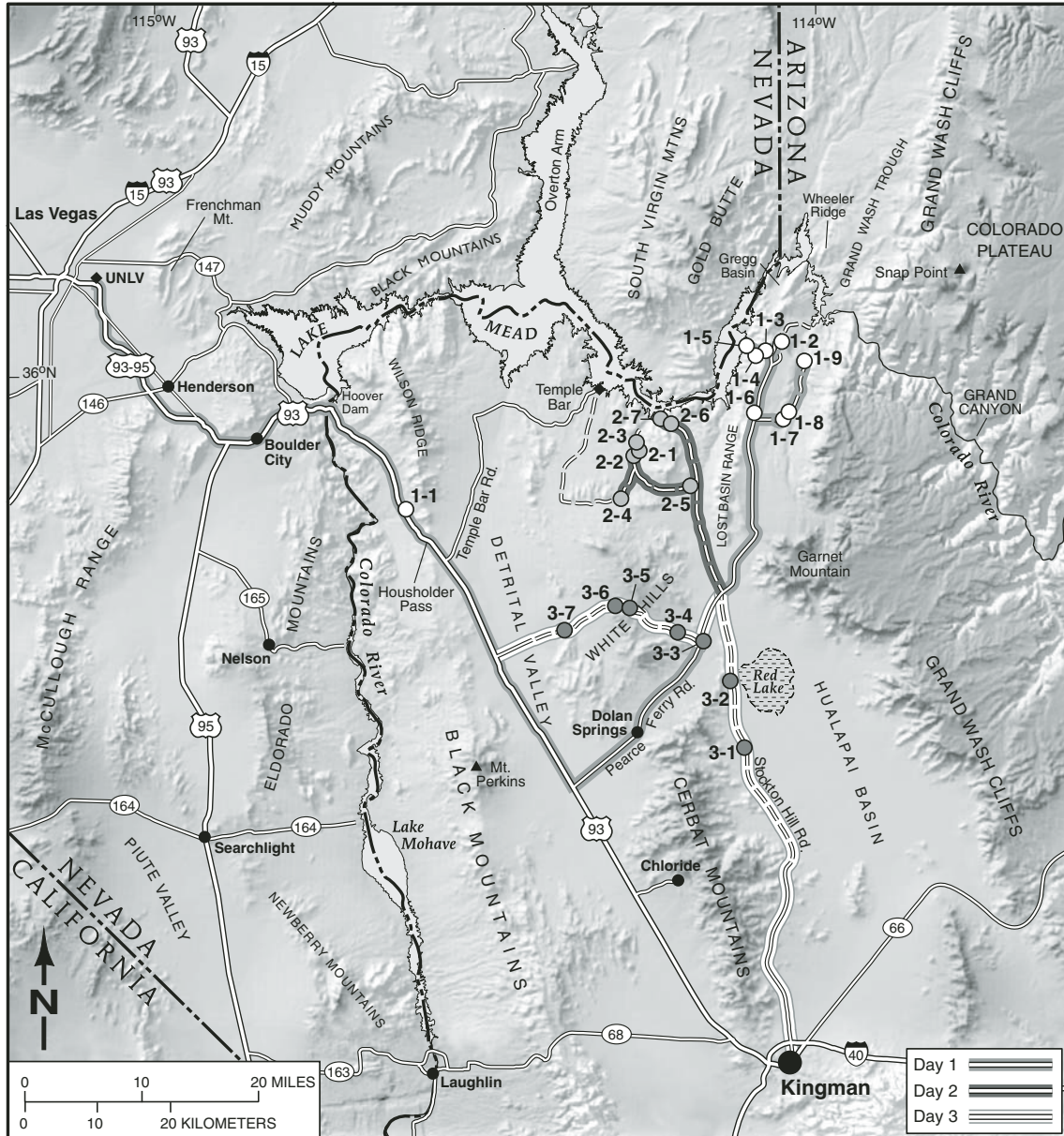


Figure 3. Map showing field trip route for each day and major physiographic features in the northern Colorado River extensional corridor and neighboring parts of the western margin of the Colorado Plateau.

## REGIONAL GEOLOGIC SETTING

Northwestern Arizona and southern Nevada have occupied a critical position in the western Cordillera since Mesozoic time. In Cretaceous to early Tertiary time, this region marked the northern edge of a large crystalline terrane referred to as the Kingman uplift (Goetz et al., 1975) or Kingman arch (Bohannon, 1984), which was stripped of its Paleozoic and Mesozoic cover by erosion during Paleogene time. Later, during the middle to late Tertiary, the Lake Mead region marked the northern end of the highly extended Colorado River extensional corridor, which

was dominated by ~east-west extension (e.g., Davis et al., 1980; Howard and John, 1987; Davis and Lister 1988; Faulds et al., 1990, 2001a; Campbell and John, 1996). In contrast, the region directly north of Lake Mead was characterized by a complex three-dimensional strain field involving strike-slip faulting and north-south shortening, in addition to large-magnitude ~east-west extension (e.g., Weber and Smith, 1987; Anderson and Barnhard, 1993; Anderson et al., 1994; Duebendorfer and Simpson, 1994).

In the northern part of the extensional corridor, calc-alkaline magmatism and major east-west extension swept northward in early to middle Miocene time (e.g., Glazner and Bartley,

1984; Gans et al., 1989; Faulds et al., 1999). Magmatism began ca. 18–20 Ma, 1–4 m.y. before the onset of major east-west extension (Faulds et al., 1995, 1999, 2002b; Gans and Bohron, 1998). Voluminous, early Miocene, generally intermediate composition magmatism was accompanied by little deformation, although mild north-south extension affected some areas (Faulds et al., 2001a). Major east-west extension then battered the region beginning ca. 16–17 Ma in the south and migrating north-northwest to the western Lake Mead region by ca. 13 Ma. Extension ended in most areas by 11–8 Ma. Tertiary extension was accommodated by mainly west-dipping normal faults and east tilting of fault blocks in the Lake Mead area (e.g., Anderson, 1971, 1978; Duebendorfer and Sharp, 1998), whereas east-dipping faults and west-tilted fault blocks dominated to the south in the Lake Mohave region (e.g., Faulds et al., 1995; Fig. 2). The boundary between these oppositely dipping normal fault systems has been referred to as the Black Mountains accommodation zone, which corresponds to a 5–10-km-wide region of intermeshing, oppositely dipping normal faults and abundant extensional folds (Faulds et al., 1990, 2001a, 2002b; Faulds and Varga, 1998; Varga et al., 2004). The east- and west-tilted domains on either side of the accommodation zone are termed the Lake Mead and Whipple domains, respectively (Spencer and Reynolds, 1989). Estimates of extension within the northern part of the corridor range from ~75%–100% (e.g., Faulds et al., 1990; Brady et al., 2000).

Thick sections (generally >3 km) of Tertiary volcanic and sedimentary strata rest directly on Proterozoic and late Cretaceous metamorphic and plutonic rock within the bulk of the extensional corridor (Anderson, 1971; Sherrod and Nielson, 1993; Faulds et al., 1995, 2002b; Beard, 1996). Sections are thickest in middle to late Miocene half grabens. The strata typically range in age from early to late Miocene and consist of mafic to felsic lavas, ash-flow tuffs, clastic sedimentary rocks, rock avalanche deposits, volcanic breccia, and evaporites. Although preserved to the north, east, and west of the region, Paleozoic and Mesozoic strata are missing from all but the northernmost part of the extensional corridor (i.e., Lake Mead region) owing to significant early Tertiary erosion of the Kingman arch. Basement rocks include Paleoproterozoic gneisses, ca. 1.4 Ga granite, Late Cretaceous–early Tertiary peraluminous (two-mica and garnet-bearing) granites, and early to middle Miocene silicic to intermediate plutons and mafic to felsic dike swarms.

During extension, older units were progressively tilted to steeper dips concurrent with deposition of younger sequences on subhorizontal surfaces. Consequently, many of the basins contain well-developed tilt fanning (i.e., growth-fault sequences), whereby tilts within the synextensional parts of the section progressively decrease upwards. Volcanic units in many half grabens permit precise dating of the timing of extension (e.g., Faulds et al., 1995, 1999, 2002b; Duebendorfer and Sharp, 1998; Gans and Bohron, 1998; Varga et al., 2004). Tilt fanning indicates that major east-west extension began 16.7–15.7 Ma and continued at high rates until ca. 13 Ma in a broad region of the corridor extending from the latitude of Kingman, Arizona, on the south to the eastern Lake

Mead region on the north (Anderson et al., 1972; Beard, 1996; Faulds et al., 1995, 1999, 2002b; Duebendorfer and Sharp, 1998). Major extension then shifted northwestward ca. 13 Ma into the western Lake Mead region, where it continued until ca. 9 Ma (Duebendorfer and Wallin, 1991; Harlan et al., 1998; Castor et al., 2000). Since ca. 8 Ma, the northern Colorado River extensional corridor has experienced only minor tilting and faulting.

In contrast to the extensional corridor, the Colorado Plateau has remained tectonically stable through Cenozoic time and is essentially unextended at upper-crustal levels, as evidenced by subhorizontal Paleozoic and Mesozoic strata. Approximately 2 km of Paleozoic and Mesozoic strata caps the Colorado Plateau but is absent in much of the Basin and Range province of central and western Arizona (Peirce, 1985; Lucchitta and Young, 1986). Late Cretaceous marine deposits on the Colorado Plateau (Nations, 1989) suggest nearly 2 km of uplift during Cenozoic time (Parsons and McCarthy, 1995). However, the timing and nature of Colorado Plateau uplift remain controversial, because the transition zone and much of the Basin and Range province are structurally higher than the Colorado Plateau. Thus, both the Basin and Range and Colorado Plateau may have originally been uplifted, perhaps in early Tertiary time, but parts of the Basin and Range province later subsided. The border between the Colorado Plateau and Basin and Range is generally marked by a broad (~50–150 km wide) transition zone containing characteristics of both provinces (Peirce, 1985). In northwestern Arizona, however, an abrupt boundary separates the relatively unextended Colorado Plateau and Basin and Range province (Figs. 1 and 2). Large Miocene half grabens along the eastern margin of the Colorado River extensional corridor chronicle the evolution of this tectonic boundary and also elucidate major events that facilitated development of the Colorado River.

## A TALE OF THREE BASINS

In this section, we describe three major basins along the eastern margin of the Colorado River extensional corridor: the Grand Wash trough, White Hills basin, and Hualapai basin. The Grand Wash trough and White Hills basin are complex, composite east-tilted half grabens, whereas the Hualapai basin is a relatively simple east-tilted half graben. Neogene deposits within each of these half grabens have important implications for understanding the tectonic and paleogeographic evolution of this region.  $^{40}\text{Ar}/^{39}\text{Ar}$  geochronology and geochemical correlations of tephros (tephrochronology) constrain the timing of deformation in both the Grand Wash trough and White Hills basin. The field trip will visit the Grand Wash trough on Day 1, northern White Hills basin on Day 2, and southern White Hills and Hualapai basins on Day 3.

### Grand Wash Trough (Day 1)

The Grand Wash trough consists of at least two east-tilted half grabens, which are separated by Wheeler Ridge in the north and the Lost Basin Range in the south (Fig. 2). The eastern half

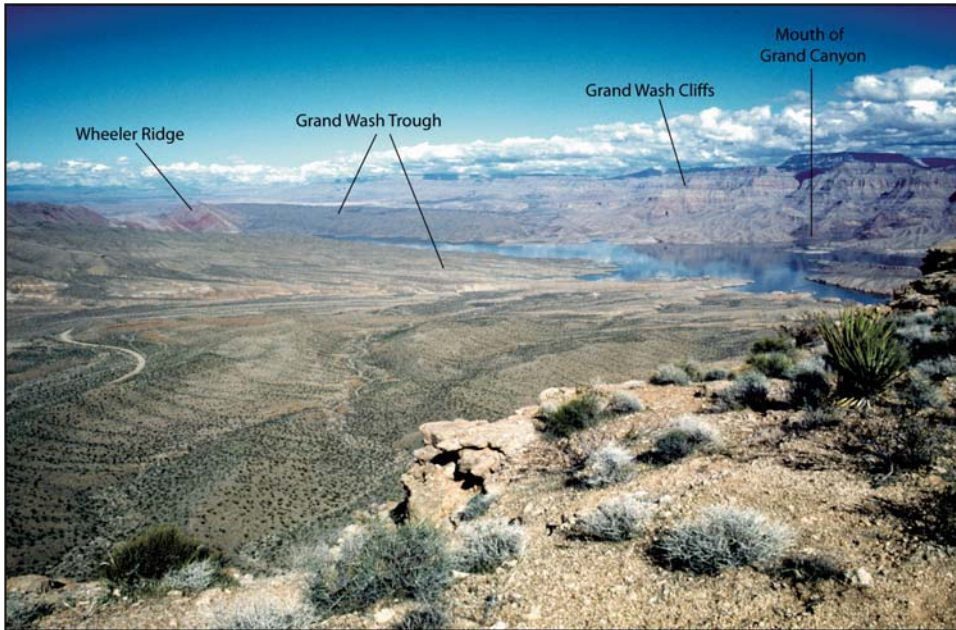


Figure 4. View looking north at the Grand Wash trough, Grand Wash Cliffs, and Wheeler Ridge from Airport Point at the north end of Grapevine Mesa. Note the contrast between the subhorizontal strata along the Grand Wash Cliffs and steeply east-dipping strata on Wheeler Ridge.

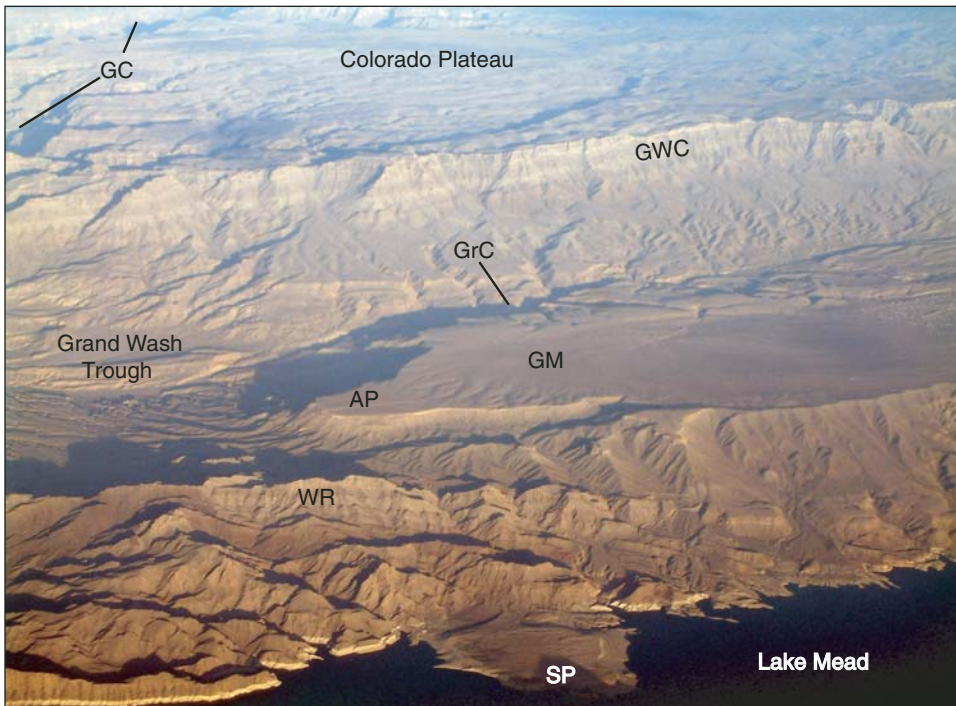


Figure 5. View looking east of the Grand Wash trough and western margin of the Colorado Plateau, including Airport Point (AP), Grand Canyon (GC), Grand Wash Cliffs (GWC), Grapevine Mesa (GM), which is capped by the Hualapai Limestone), Grapevine Canyon (GrC), Sandy Point (SP), and Wheeler Ridge (WR). Grapevine Mesa essentially marks the floor of a late Miocene lake that immediately predates arrival of the Colorado River. Also, note the gentle northeast dip of Paleozoic strata along the Grand Wash Cliffs.

graben developed in the hanging wall of the west-dipping northern Grand Wash fault and is centered in the Grapevine Wash area. To the west, the Gregg Basin is a relatively narrow east-tilted half graben that lies in the hanging wall of the west-dipping Wheeler Ridge and Lost Basin Range faults. The Wheeler Ridge and Lost Basin Range faults probably represent splays of the Grand Wash fault zone. As Wheeler Ridge dies out to the north of Lake Mead, the two half grabens coalesce to form a large composite basin, at least at exposed levels. Dissection by the Colorado River and its tributaries has produced excellent exposures of the upper part of the Tertiary section in both the Grand Wash trough and Gregg Basin (Figs. 4 and 5).

The middle to late Miocene section within the Grand Wash trough (referred to as the rocks of the Grand Wash trough after Bohannon, 1984) includes, in ascending order, at least 250 m of middle to late Miocene fanglomerate, more than 120 m of a sandstone-siltstone facies with locally interbedded gypsum, and as much as 300 m of late Miocene limestone (Figs. 6 and 7A; Longwell, 1936; Lucchitta, 1966; Bohannon, 1984; Wallace,

1999; Wallace et al., 2005; Blythe, 2005). The units interfinger and thicken eastward toward the deeper parts of the half graben. The conglomerate contains many large boulders (>5 m long) of the 1.4 Ga Gold Butte Granite (e.g., Volborth, 1962; Silver et al., 1977), a megacrystic rapakivi granite derived from the Gold Butte block in the south Virgin Mountains ~6–10 km to the west (Longwell, 1936; Lucchitta, 1966; Lucchitta and Young, 1986; Wallace, 1999; Blythe, 2005). The limestone in the Grand Wash trough is known as the Hualapai Limestone and has been correlated with similar limestone elsewhere in the eastern Lake Mead region (Longwell, 1928, 1936; Lucchitta, 1966). It has been interpreted as either marine (Blair, 1978; Blair and Armstrong, 1979) or non-marine (Lucchitta, 1966; Faulds et al., 1997; Wallace, 1999).

The rocks of the Grand Wash trough are bracketed between ca. 15 and 6 Ma. The older age is based on a 15.3 Ma  $^{40}\text{Ar}/^{39}\text{Ar}$  date on sanidine from a rhyolite tuff near the base of the section on the west flank of Grapevine Mesa (Faulds et al., 2001b). Younger age constraints include (1) an 8.8 Ma basalt flow (Faulds et al., 2001b) intercalated with alluvial fan deposits shed from the

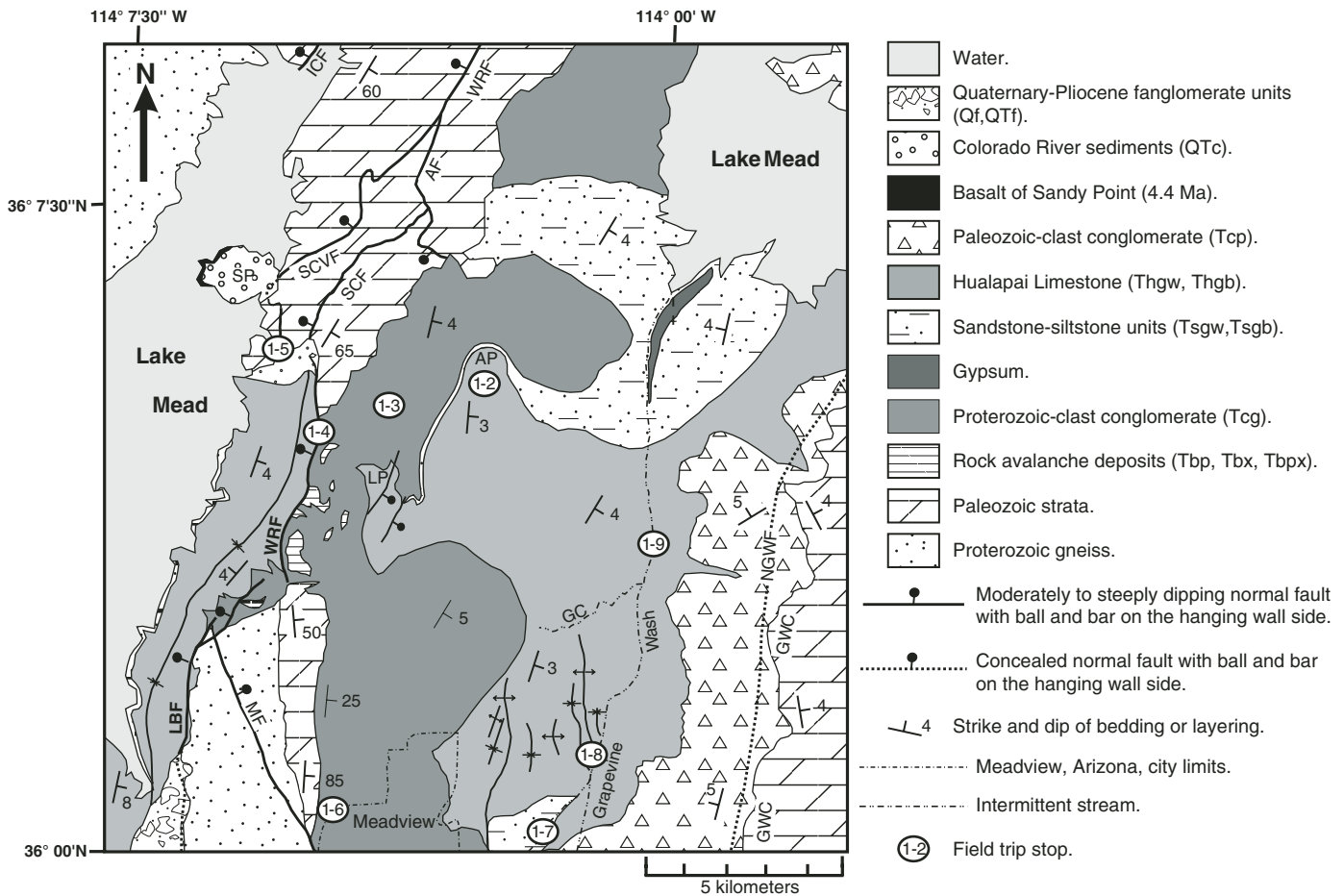


Figure 6. Generalized geologic map for the Grand Wash trough, showing field trip stops. AF—Airport fault; AP—Airport Point; GC—Grapevine Canyon; GWC—Grand Wash Cliffs; ICF—Iceberg Canyon fault; LBF—Lost Basin Range fault; LP—Lookout Point; MF—Meadview fault; NGWF—northern Grand Wash fault; SCF—Sheep Canyon fault; SCVF—South Cove fault; SP—Sandy Point; WRF—Wheeler Ridge fault.

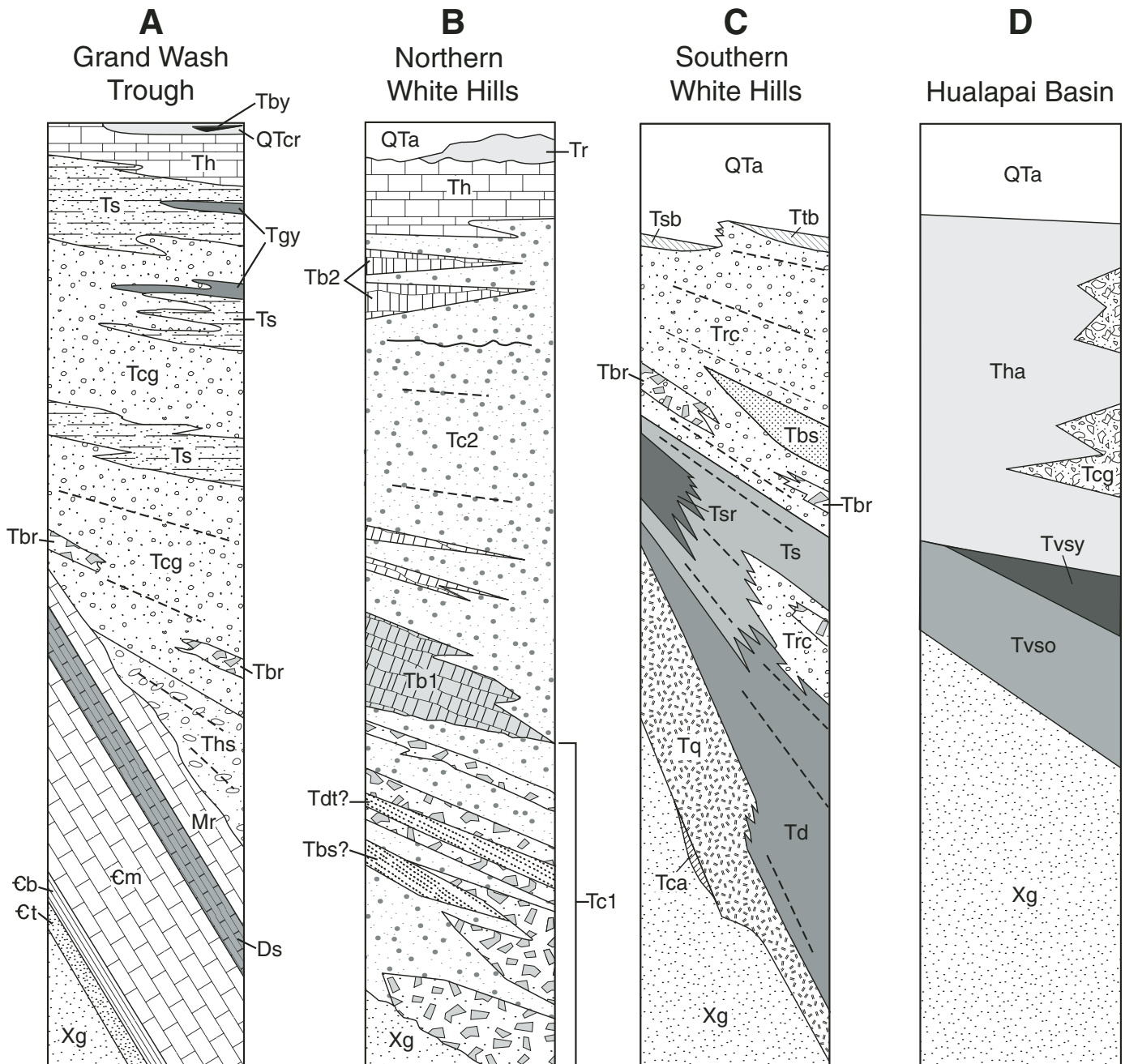


Figure 7. Generalized stratigraphic columns of major basins near the eastern margin of the northern Colorado River extensional corridor, showing approximate tilts and relative unit thicknesses. (A) Grand Wash trough. QTc—Colorado River sediments; Tby—early Pliocene basalts (e.g., 4.4 Ma Sandy Point basalt; Th, 11–6 Ma Hualapai Limestone; Ts—Sandstone-siltstone facies; Tgy—gypsum; Tcg—conglomerate derived from Gold Butte block; Tbr—megabreccia of Proterozoic or Paleozoic rock; Ths—tuffaceous sedimentary rocks probably correlative with Horse Spring Formation (e.g., Beard, 1996) and containing a 15.3 Ma tuff (Faulds et al., 2001b); Mr—Redwall Limestone; Ds—Sultan Limestone; Cm—Muav Limestone; Cb—Bright Angel Formation; Ct—Tapeats Sandstone; Xg—Paleoproterozoic gneiss. (B) Northern White Hills basin. See map (Fig. 10) for letter symbols. QTa—late Miocene-Quaternary basin-fill sediments; Tr—rounded gravel, sand, and silt; Th—Hualapai Limestone; Tc2—angular, poorly sorted sand and gravel, which has yielded dates from ca. 14.4–10.9 Ma (Blythe, 2005); Tb2—olivine basalt dated 8.3 Ma (Beard et al., 2007); Tb1—lower basaltic flows dated ca. 14.6 Ma (Duebendorfer and Sharp, 1998); Tc1—angular, poorly sorted sandy gravel (granular pattern) and lenses of megabreccia (blocky pattern); Tdt?—ash-flow tuff intercalated with megabreccia and poorly sorted angular conglomerate in Tc1, dated as 15.2 Ma (Duebendorfer and Sharp, 1998), may correlate with the tuff of Mt Davis (e.g., Faulds et al., 2002b); Tbs?—ash-flow tuff that may correlate with the tuff of Bridge Spring (e.g., Faulds et al., 2002b); Xg—Proterozoic gneiss. (C) Southern White Hills basin. Patterns and labels are the same as in Figure 11 except Tbr (megabreccia of Proterozoic rock). (D) Hualapai basin: QTa—Holocene-late Miocene shale, conglomerate, gypsum, and anhydrite; Tha—late Miocene (probably ca. 13–8 Ma) halite and lesser shale and anhydrite; Tcg—locally derived late Miocene conglomerate; Tvsy—middle Miocene (ca. 16–13 Ma) volcanic and sedimentary rock; Tvso—early to middle Miocene (ca. 20–16 Ma) volcanic and sedimentary rock, possibly resting on a thin section of Cambrian strata; Xg—Proterozoic gneiss, granite, and diabase.

Grand Wash Cliffs at Nevershine Mesa (Lucchitta et al., 1986) in the northern part of the trough; (2) a  $7.43 \pm 0.22$  Ma  $^{40}\text{Ar}/^{39}\text{Ar}$  maximum eruptive age on sanidine from an ash-fall tuff intercalated in the upper part of the Hualapai Limestone at Grapevine Mesa (Wallace et al., 2005); and (3) a 6.0 Ma tephra within the upper Hualapai Limestone in the Temple Bar area to the west of the Grand Wash trough (Spencer et al., 2001).

Tilting within the rocks of the Grand Wash trough decreases up-section from  $\sim 30^\circ$  in the lowermost ca. 15 Ma units to  $< 5^\circ$  in the youngest units (ca. 4.4–6 Ma). The gently to moderately tilted ( $< 30^\circ$ ) lower conglomerate onlaps moderately to steeply ( $40\text{--}90^\circ$ ) east-tilted Paleozoic strata and Proterozoic gneiss at Wheeler Ridge and in the Lost Basin Range, respectively. The late Tertiary section (ca. 13–4.4 Ma) is generally tilted gently eastward ( $< 10^\circ$ ). The Hualapai Limestone onlaps subhorizontal Paleozoic strata along the Grand Wash Cliffs; its upper part is not cut by the northern Grand Wash fault. In contrast, the Wheeler Ridge fault accommodated  $\sim 300$  m of offset of the Hualapai Limestone (Fig. 8; Lucchitta, 1966; Wallace et al., 2005), gentle tilting of early Pliocene basalts and Colorado River sediments (Howard et al., 2000), and appears to cut early Pleistocene alluvial fan deposits (Wallace et al., 2005). These relations indicate that major extension in the Grand Wash trough began prior to 15.3 Ma and that the main pulse of extension had ended by ca. 13 Ma. Movement on the northern Grand Wash fault had ceased by 6 Ma; however, activity on the Wheeler Ridge fault continued into at least the early Pliocene and possibly Quaternary time.

The rocks of the Grand Wash trough have significant paleogeographic implications (Lucchitta, 1966, 1979). For example, the timing of possible uplift of the Colorado Plateau during late Cenozoic time (McKee and McKee, 1972) has been extrapolated

from studies of basinal sedimentary deposits within the Grand Wash trough and elsewhere within the lower Colorado River region (Lucchitta, 1979). The westerly provenance of the lower conglomerate unit indicates that no major through-going drainages flowed westward from the Colorado Plateau between ca. 15.3 and 11 Ma. The Hualapai Limestone is also important, as it crops out throughout much of the Lake Mead region proximal to the present course of the Colorado River (Fig. 9). Lucchitta (1966) characterized the limestone as lacustrine based on facies relationships with detrital rocks in the Grand Wash trough. In contrast, Blair (1978), Blair and Armstrong (1979), and Bradbury and Blair (1979) used fossil assemblages, petrography, and  $\delta^{13}\text{C}$  isotopic chemistry to interpret the Hualapai Limestone as marine-estuarine. They further concluded that the Hualapai Limestone marked the northern extent of an ancestral Gulf of California. Because no significant late Miocene to recent faulting was documented between the Grand Canyon and lower Colorado River regions, Lucchitta (1979) concluded that the Hualapai Limestone and the presumably marine or estuarine Bouse Formation (e.g., Metzger, 1968; Smith, 1970; Busing, 1990) in the lower Colorado River region were similar in age and deposited at approximately the same elevations (sea level or below). These deposits were therefore used to support 400–900 m of Pliocene–Quaternary uplift of the Colorado River extensional corridor and western part of the Colorado Plateau (Lucchitta, 1979, 1998). This uplift presumably induced rapid down-cutting of the Grand Canyon by the Colorado River since 6 Ma (Lucchitta, 1979, 1989).

Recent studies, however, have raised serious questions about these interpretations. For example, Spencer and Patchett (1997) concluded on the basis of  $^{87}\text{Sr}/^{86}\text{Sr}$  isotopic evidence that carbonates within the late Miocene to Pliocene Bouse Formation

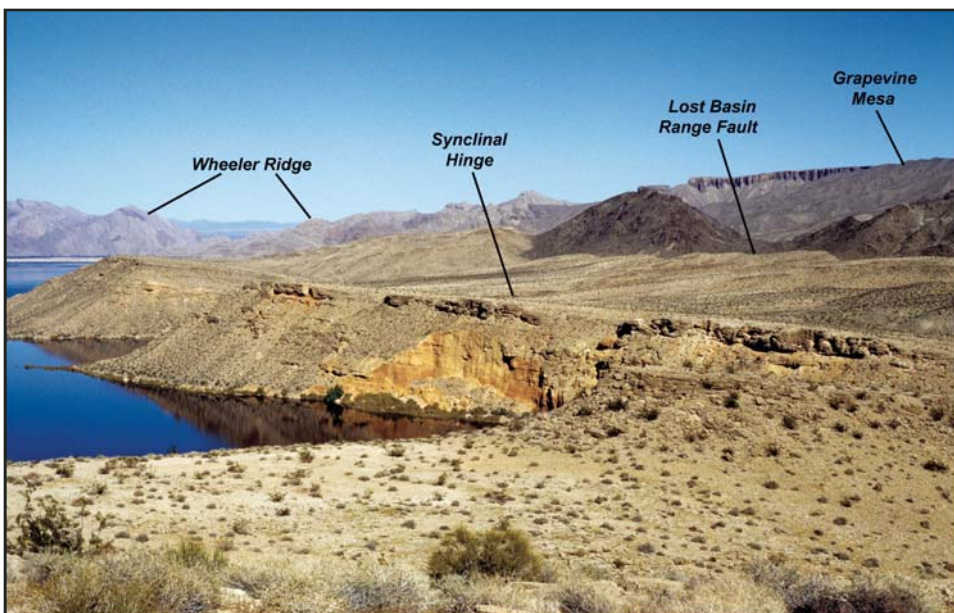


Figure 8. View northeast of Gregg Basin syncline and faulted Hualapai Limestone. This syncline results from east-tilting of the Gregg Basin half graben and normal drag along the west-dipping Wheeler Ridge and Lost Basin Range faults. Thus, it is extensional in origin.

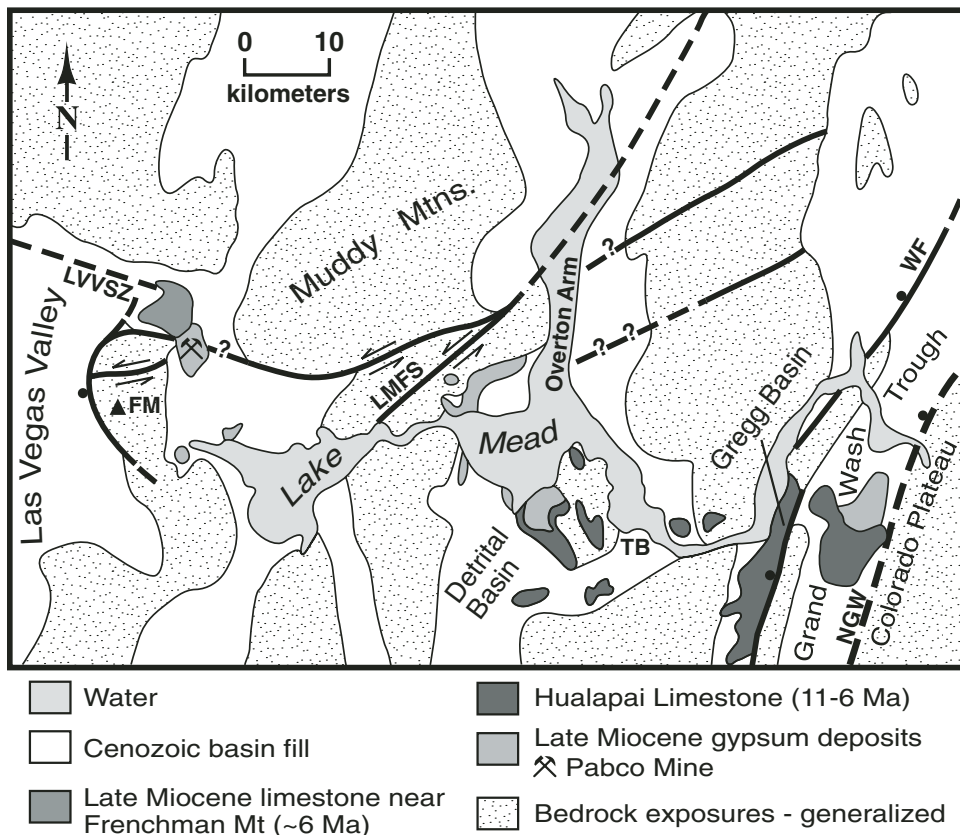


Figure 9. Generalized geologic map showing distribution of late Miocene limestone and gypsum deposits in the Lake Mead area. The limestones are all lacustrine and found proximal to the present course of the Colorado River, suggesting that the source of fresh water for the limestones may have been derived from a drainage network (surface water and/or groundwater) that ultimately evolved into the Colorado River. The presence of late Miocene gypsum in most of these basins beneath the limestone and thick salt deposits in some of the neighboring basins (e.g., Overton Arm, Detrital, and Hualapai basins) further suggests that large playas existed just prior to limestone deposition and possibly adjacent to some of the freshwater lakes during limestone deposition. FM—Frenchman Mountain; LMFS—Lake Mead fault system; LVSZ—Las Vegas Valley shear zone; NGW—northern Grand Wash fault; TB—Temple Bar; WF—Wheeler Ridge fault.

in the lower Colorado River region and the Hualapai Limestone near Temple Bar are lacustrine in origin. Furthermore, evidence from fossil assemblages, petrography, and  $\delta^{13}\text{C}$ – $\delta^{18}\text{O}$  isotopic geochemistry clearly support a nonmarine (lacustrine) origin for the Hualapai Limestone (Wallace, 1999; Faulds et al., 2001c; Wallace et al., 2005). If not marine or estuarine, the limestone within the Lake Mead and lower Colorado River regions cannot be used as evidence to support (1) late Miocene to recent uplift of the southwestern Colorado Plateau, (2) the northern extent of the ancestral Gulf of California, or (3) rapid down-cutting of the Grand Canyon since 6 Ma.

### White Hills Basin (Days 2 and 3)

A large structural block exposing Proterozoic basement separates much of the Grand Wash trough from basins to the west (Fig. 2). From north to south, this 75-km-long block consists of the Gold Butte block, Hiller Mountains, and White Hills, all forming the footwall to the major west-dipping South Virgin–White Hills detachment fault. The White Hills basin is a large northerly trending group of east-dipping half grabens developed in the hanging wall of the South Virgin–White Hills detachment fault. Although the South Virgin–White Hills detachment has a sinuous trace in the White Hills and is marked by several prominent salients and embayments, a more or less continuous basin

appears to characterize the hanging wall. However, to date, only the northern and southern parts of this presumably continuous basin have been studied in detail. Because these areas contain notable stratigraphic differences, we describe them separately below as the northern and southern White Hills basins.

### Northern White Hills Basin (Day 2)

The hanging wall of the South Virgin–White Hills detachment fault in the northern White Hills exposes tilted middle to upper Miocene fanglomerate, megabreccia, and volcanic rocks bracketed between 15.2 and ca. 10 Ma, for which upward-decreasing dips indicate deposition during movement on the detachment fault (Duebendorfer and Sharp, 1998; Blythe, 2005; Figs. 7B and 10). They and the South Virgin–White Hills detachment fault are overlain unconformably by upper Miocene fanglomerate, olivine basalt flows, and the Hualapai Limestone, as young as 6.0 Ma. Gypsum and mudstone indicate a depocenter in the western part of the basin, in the Virgin–Detrital trough (Longwell, 1936; Beard et al., 2007). The Hualapai Limestone is the youngest basin fill predating the arrival of and incision by the Colorado River.

Two unconformity-bounded sequences comprise the hanging-wall strata of the South Virgin–White Hills detachment fault in Salt Spring Wash, which contains the best exposures of the northern White Hills basin. The lower sequence is juxtaposed directly against highly retrograded crystalline footwall rocks along the

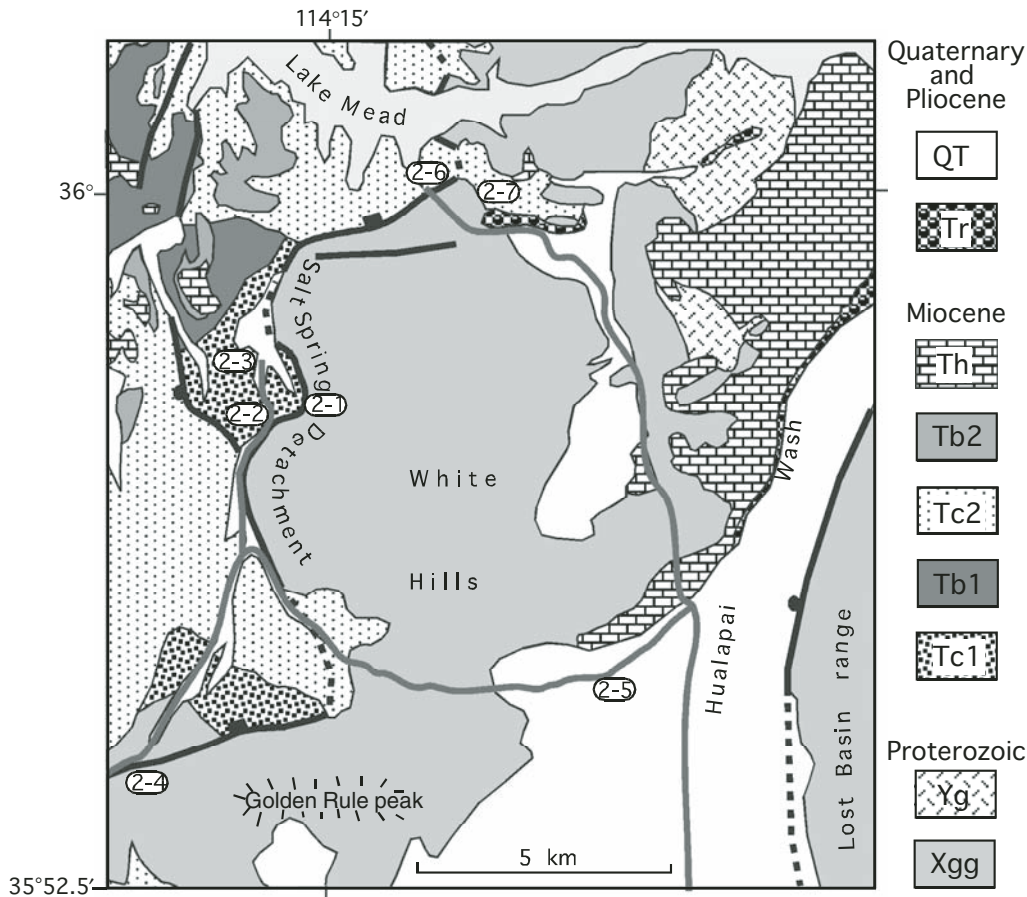


Figure 10. Generalized map of Salt Spring Wash area. Salt Spring detachment fault is a segment of the South Virgin–White Hills detachment fault. QT—Alluvium (Quaternary and Pliocene); Tr—Ancestral Colorado River deposits (Pliocene); Th—Hualapai Limestone (upper Miocene); Tb2—Olivine basalt (upper Miocene); Tc2—Conglomerate (upper to middle Miocene); Tb1—Pyroxene basaltic andesite (middle Miocene); Tc1—Conglomerate, megabreccia, and tuff (middle Miocene); Yg—Gold Butte Granite (Mesoproterozoic); Xgg—Gneiss and granite (Paleoproterozoic).

South Virgin–White Hills detachment. This section consists of fanglomerate and megabreccia intercalated with a tuff dated at 15.2 Ma (Duebendorfer and Sharp, 1998). The largest single megabreccia block is >200 m thick, can be traced for >1000 m along strike, and appears to have been derived from the footwall of the South Virgin–White Hills detachment fault. Tilts within this lower sequence range from ~30° to 60°. These rocks are overlain along an angular unconformity by the upper sequence, an interbedded basalt-fanglomerate section that thickens to the north and west. The basal unit of the upper sequence is a basaltic andesite dated 14.6 Ma (Duebendorfer and Sharp, 1998). Similar mafic volcanic rocks of this sequence thicken westward in the basin toward the northwestern White Hills, where they have yielded dates of 14.8–14.4 Ma (Cascadden, 1991; Beard et al., 2007). The fanglomerates, which overlie and interfinger with the basaltic andesite, fan upward in dip and have been dated between ca. 14.4 and 10.9 Ma on tuff interbeds (Blythe, 2005). A correlative megabreccia deposit in the northern part of the basin is as thick as 120 m, contains blocks as long as 30 m, and dips back toward the Gold Butte block, from which the clasts were derived (Longwell, 1936).

The hanging-wall basin thus records debris including rock avalanches shed from the Proterozoic rocks in the footwall block of the South Virgin–White Hills detachment fault while the fault

was active. Where exposed, the fault dips from 45° to as little as 16°. The fault cuts sediments estimated as young as ca. 10–12 Ma, the dips of which roll into the fault (Howard et al., 2003; Blythe, 2005). Based on the dips of enclosing fanglomerates, the South Virgin–White Hills detachment fault ceased activity after deposition of tuffs dated 12.0 and ca. 10.9 Ma (Blythe, 2005) and earlier than a basalt flow dated 8.4 Ma (Beard et al., 2007). Overlying little-deformed, upper Miocene fanglomerate and the Hualapai Limestone lap onto the footwall block, where they fill paleovalleys cut into Proterozoic rocks and bridge across the block to connect with the Gregg Basin on the east (Howard et al., 2003). The interior basins therefore filled during and after faulting on the South Virgin–White Hills detachment fault until the fills rose to levels that connected the basins across low parts of the large footwall massif. Some of the resulting interbasin sedimentary connections were later occupied by paths of the Pliocene Colorado River, when this regional stream developed across the region (Howard et al., 2008).

#### **Southern White Hills Basin (Day 3)**

The southern White Hills basin is a large, composite, east-tilted half graben in the hanging wall of the Cyclopic fault and northern part of the Cerbat Mountains fault (Fig. 11; Price, 1997;

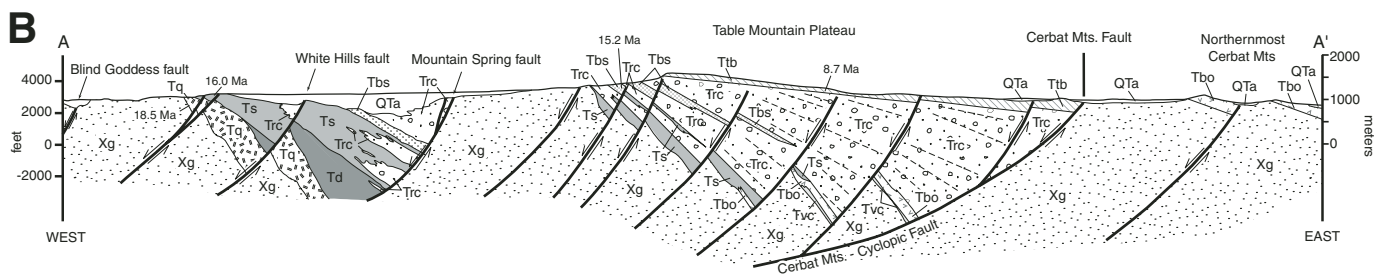
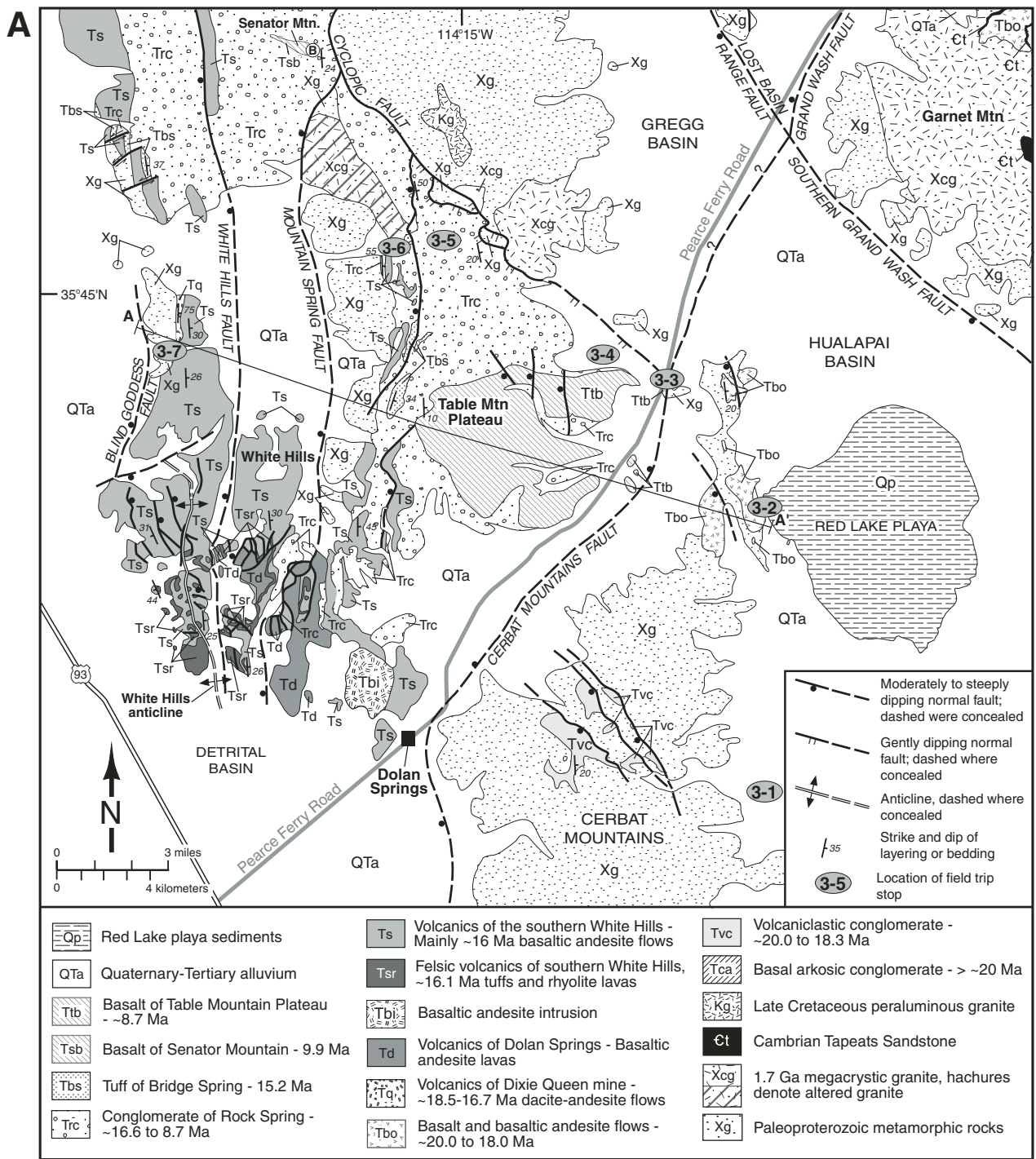


Figure 11. (A) Generalized geologic map of the southern White Hills and adjacent areas. (B) Cross section A–A', shown slightly larger than map scale for ease of viewing but with no vertical exaggeration. The conglomerate of Rock Spring is a thick synextensional unit that thickens eastward in the eastern subbasin of the southern White Hills basin. Note that tilts progressively decrease upward between the upper part of the volcanics of Dolan Springs and basalt of Table Mountain Plateau. Greater tilting within the hanging wall indicates a listric geometry for the Cerbat Mountains and Cyclopic fault zones, which probably merge at depth beneath the eastern subbasin.

Faulds et al., 2001b), which collectively mark the southern part of the South Virgin–White Hills detachment fault. As much as 3 km of Miocene volcanic and sedimentary strata accumulated on an erosion surface etched into Paleoproterozoic gneiss and granite, as well as Late Cretaceous peraluminous granite. In ascending order, the stratigraphy in the southern White Hills includes (Fig. 7C) (1) 18.5 to ca. 16 Ma trachydacite-trachyandesite lavas of the volcanics of Dixie Queen Mine (cf. Faulds et al., 1995); (2) basaltic andesite lavas of the volcanics of Dolan Springs; (3) a ca. 16 Ma bimodal sequence of intercalated rhyolite lavas, tuffs, and basaltic andesite flows, referred to as the volcanics of the southern White Hills; (4) the 15.2 Ma tuff of Bridge Spring (cf. Morikawa, 1994; Faulds et al., 1995, 2002b); (5) ca. 16–8.7 Ma synextensional fanglomerates, referred to as the conglomerate of Rock Spring; and (6) 8.7 Ma basalt of Table Mountain Plateau and 9.9 Ma basalt of Senator Mountain.

The northerly striking Mountain Spring fault separates the southern White Hills into two distinct lithologic domains, or subbasins (Fig. 11). In the eastern subbasin, thick sections of fanglomerate (conglomerate of Rock Spring) and subordinate volcanic units accumulated in an eastward-thickening wedge bounded by the Cerbat Mountains and Cyclopic faults on the east. In contrast, volcanic rocks dominate the southern and central parts of the western subbasin, which developed in the mutual hanging walls of the Mountain Spring, Cerbat Mountains, and Cyclopic faults. As the volcanic section thins to the north in the northern part of the southern White Hills, however, the distinction between the eastern and western subbasins becomes less conspicuous. The large volcanic component in the western subbasin is more characteristic of half grabens within the bulk of the northern Colorado River extensional corridor (e.g., Anderson, 1971, 1978; Faulds, 1996; Faulds et al., 1995, 2001a, 2002b) and contrasts with the sediment-dominated basins along the eastern margin of the corridor and in the Lake Mead area (e.g., Lucchitta, 1966; Bohannon, 1984; Beard, 1996; Faulds et al., 1997, 2001c).

The timing of extension within the southern White Hills is bracketed between ca. 16.7 and 8 Ma. Tilts within the southern White Hills progressively decrease up-section from  $\sim 75^\circ$  in the volcanics of Dixie Queen Mine to  $\sim 5^\circ$  in the basaltic lavas of Table Mountain Plateau (Fig. 12). Major east-west extension probably began ca. 16.7–16.2 Ma during deposition of the lowermost part of the conglomerate of Rock Spring, as evidenced by clasts of Proterozoic gneiss likely derived from surrounding footwall blocks. Although not fully exposed in any single fault block in the southern White Hills, concordant tilts in exposed parts of the lower Miocene section within individual fault blocks indicate little tilting and extension prior to ca. 16.7 Ma. Extension was clearly in full swing, however, during eruption of the ca. 16 Ma volcanics of the southern White Hills, as evidenced by angular unconformities with older units and appreciable tilt fanning (tilts decrease up-section from  $\sim 50^\circ$  to  $25^\circ$ ) (Figs. 11 and 12). Tilt fanning suggests that peak extension occurred between ca. 16.5 and 15 Ma. The final stages of extension are recorded by minor faulting and gentle tilting of the 8.7 Ma basalts. Although no evidence

for Quaternary faulting was observed in the southern White Hills, it is possible that some of the faulting temporally correlates with that in the eastern Lake Mead area and may therefore be younger than ca. 6 Ma.

The conglomerate of Rock Spring is a particularly important unit in the southern White Hills for elucidating the paleogeographic evolution of the region. It accumulated primarily in the eastern subbasin of the southern White Hills basin east of the Mountain Spring fault (Fig. 11). The conglomerate is bracketed between ca. 16.7 and 8.7 Ma by  $^{40}\text{Ar}/^{39}\text{Ar}$  ages on underlying and overlying volcanic units. Clasts of Proterozoic gneiss and megacrystic granite, ranging up to  $\sim 10$  m long, dominate the conglomerates. The matrix-supported texture, subangular clasts, and poor sorting suggest a fanglomerate origin for the conglomerate. The conglomerate forms an eastward-thickening wedge-shaped body in the southern White Hills and is as much as 2.6 km thick proximal to the Cerbat Mountains fault (Fig. 11). The conglomerate of Rock Spring probably correlates with similar conglomerate and rock avalanche deposits in the hanging wall of the northern White Hills basin, where Duebendorfer and Sharp (1998) documented thick middle Miocene rock-avalanche deposits of Proterozoic gneiss derived from the footwall of the detachment.

Likely sources for the boulders of megacrystic Proterozoic granite in the conglomerate of Rock Spring include the southern footwall of the Cyclopic Mine fault and Garnet Mountain  $\sim 15$  km to the east along the western margin of the Colorado Plateau (Figs. 2, 3, and 11). The relatively small body of megacrystic granite in the footwall of the Cyclopic fault, compared to the much larger body at Garnet Mountain, and the abundance of megacrystic granitic clasts within the entire 2.6-km-thick section of conglomerate of Rock Springs suggest that Garnet Mountain was a source for at least some of the detritus. Thus, the conglomerate of Rock Spring may record west-flowing drainages eroding headward into the footwall of the South Virgin–White Hills detachment fault and possibly into the western margin of the Colorado Plateau as early as ca. 16 Ma, essentially at the onset of major east-west extension.

### **Hualapai Basin (Day 3)**

The Hualapai basin is a gently to moderately east-tilted half graben developed in the hanging wall of the southern Grand Wash fault (Figs. 2 and 13). Despite its proximity to the Colorado River and Grand Canyon, the Hualapai basin remains an internally drained, closed depression. Due to a lack of dissection by tributaries of the Colorado River, synextensional middle to late Miocene strata within the basin is obscured by more recent flat-lying sediments (in contrast to the highly dissected Grand Wash trough and White Hills basin). Thus, both the stratigraphy and timing of extension cannot be directly inferred from exposures in the Hualapai basin. Nonetheless, drill-hole and seismic reflection data indicate that the Hualapai basin contains a thick ( $\sim 3.9$  km) growth-fault sequence of Miocene sedimentary and volcanic rocks, with tilts decreasing up section from  $\sim 25^\circ$  to  $0^\circ$ . As inferred from analysis of core and seismic reflection profiles, the

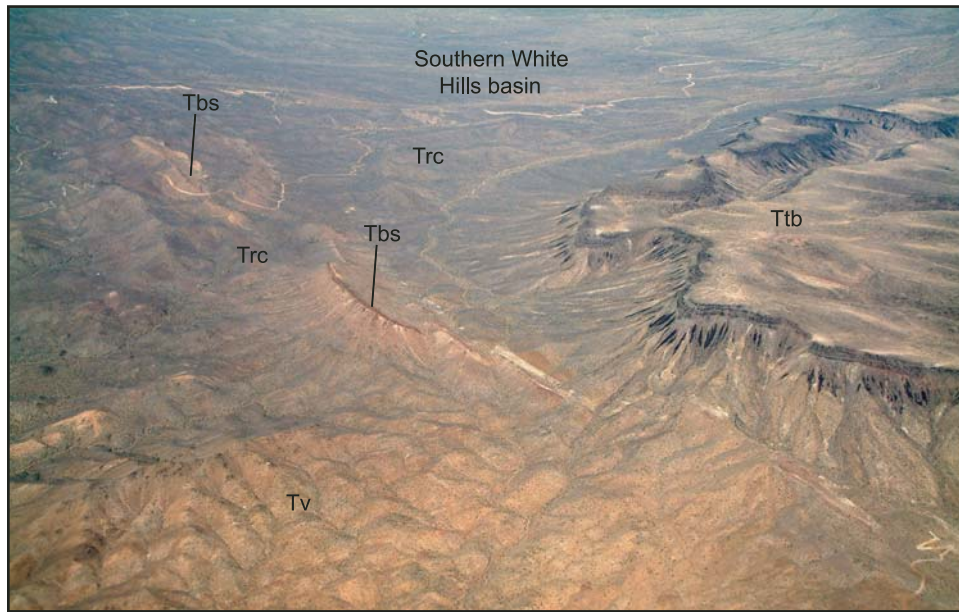


Figure 12. View to northeast of tilt fanning in southern White Hills basin. East tilts progressively decrease up-section from  $\sim 35^\circ$  in 15.2 Ma tuff of Bridge Spring (Tbs) to  $\sim 5^\circ$  in 8.7 Ma basalts of Table Mountain Plateau (Ttb). Trc—conglomerate of Rock Spring; Tv—volcanic rocks.

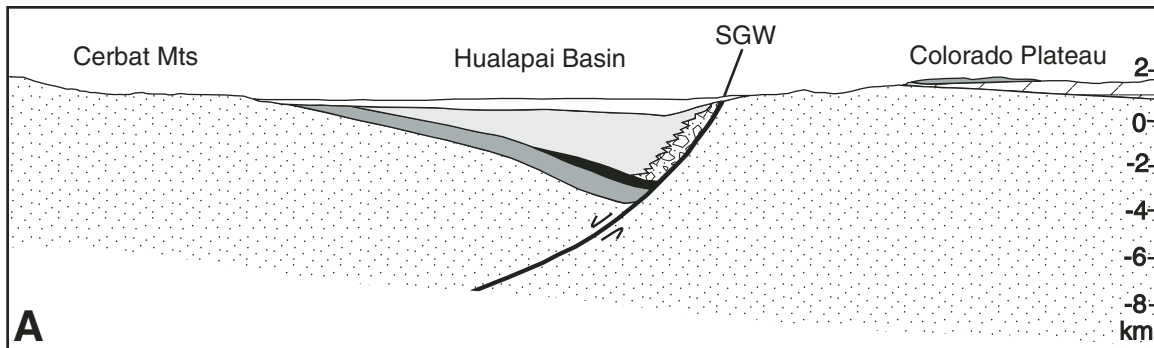


Figure 13. Hualapai basin salt deposit. The Hualapai basin contains a 2.5-km-thick nonmarine salt deposit of probable late Miocene age, as evidenced by well and seismic reflection data. (A) 1:1 cross section constrained by a migrated seismic reflection profile (from Faulds et al., 1997). Patterns for units are the same as in Figure 7D. SGW, southern Grand Wash fault. (B) Core (9 cm in diameter) showing massive halite. (C) Core showing displacive halite crystals in reddish-brown claystone. This texture indicates deposition induced by groundwater discharge in a continental playa.

stratigraphy of the Hualapai basin includes (in ascending order): (1) ~750 m of lower to middle Miocene volcanic and sedimentary rock possibly resting on Cambrian strata and/or Proterozoic gneiss, granite, and diabase; (2) ~335 m of middle Miocene volcanic and sedimentary rock; (3) fanglomerates along the margins that interfinger with evaporites in the central part of the basin; (4) up to 2500 m of middle to upper Miocene halite intercalated with minor shale (5%–10%) and anhydrite; and (5) ~600 m of late Miocene–Quaternary shale and lesser amounts of gypsum, anhydrite, and conglomerate (Faulds et al., 1997).

The Miocene section in the Hualapai basin (Fig. 7D) is dominated by the 2.5-km-thick sequence of halite, one of the thickest known, nonmarine halite deposits in a continental rift (Faulds et al., 1997). The age of the salt deposit is roughly bracketed between ca. 13 and 8 Ma, because (a) it lies in the upper, more gently tilted part ( $<10^\circ$ ) of a growth-fault sequence (Fig. 13), and (b) extension in the region peaked ca. 16–13 Ma but continued at lower rates until ca. 8 Ma. Thus, the salt temporally correlates with both the Hualapai Limestone and sandstone-siltstone facies in the Grand Wash trough, as well as with thick fanglomerates in the White Hills basin. The texture and bromine content of the halite and S and O isotopic values of intercalated and capping anhydrite indicate that halite deposition took place in an intracontinental playa that accommodated regional groundwater discharge (Faulds et al., 1997). Thick salt deposits of comparable age are also documented in the Detrital and Overton Arm basins to the west (Mannion, 1963). Thus, thick salt deposits appear to rim the central to eastern parts of the Lake Mead area. The source of the salt remains a mystery but may include chloride-rich Pennsylvanian–Permian redbeds on the Colorado Plateau (e.g., Supai Formation).

## CENOZOIC PALEOGEOGRAPHIC EVOLUTION

In early to middle Tertiary time (Paleocene through Oligocene), prior to the onset of major east-west extension, major streams flowed northeastward from the Basin and Range province onto the Colorado Plateau in northwest Arizona, as evidenced by widespread, southwesterly derived Paleocene–Eocene gravels along the western margin of the Colorado Plateau (Young, 1982). Within the northern Colorado River extensional corridor, these northeasterly flowing streams beveled the northerly trending, north-plunging Kingman arch, stripping away thick sections of Mesozoic and Paleozoic strata and exposing Proterozoic and Late Cretaceous crystalline basement. Because the arch terminated northward in the Lake Mead region, Miocene strata rest on progressively older Mesozoic and Paleozoic strata toward the south in the Lake Mead region (Bohannon, 1984) and directly overlie Proterozoic and Late Cretaceous granite and gneiss throughout most of the extensional corridor.

The distribution of the 18.5 Ma Peach Springs Tuff, a regionally extensive ignimbrite (Glazner et al., 1986; Nielson et al., 1990), indicates that major drainages in northwest Arizona continued to flow northeastward onto the Colorado Plateau through early Miocene time (Young and Brennan, 1974). The Peach

Springs Tuff probably erupted from a source near the southern tip of Nevada (Hillhouse and Wells, 1991) but is found as far east as the Grand Canyon region of the Colorado Plateau (Young and Brennan, 1974; Glazner et al., 1986; Nielson et al., 1990). In addition, sequences of presumably correlative 17–19 Ma mafic lavas crop out in both the Garnet Mountain area along the western margin of the Colorado Plateau (Lucchitta and Young, 1986; Wenrich et al., 1996) and in the northern Cerbat Mountains in the eastern part of the extensional corridor (Fig. 2; Faulds et al., 1997, 1999). Thus, in northwest Arizona and southern Nevada, including the western Grand Canyon region, the Basin and Range province was topographically higher than the Colorado Plateau, and no major structural or topographic barriers appear to have separated the two provinces as late as the early Miocene.

Middle Miocene east-west extension then fragmented the region into complex arrays of tilted fault blocks (e.g., Anderson et al., 1972; Faulds et al., 1990) and induced the topographic and structural foundering of the extensional corridor relative to the Colorado Plateau. Neogene strata within the corridor chronicle both the evolution of the Colorado Plateau–Basin and Range boundary and development of major drainage systems. Major basins began forming in the hanging walls of major west-dipping normal faults (e.g., Grand Wash fault zone) at or near the western margin of the Colorado Plateau as early as ca. 16.5 Ma. Basin development clearly disrupted the regional northeast-flowing drainage that predominated in early Tertiary time. This is particularly evident in the southern White Hills basin by the thick accumulation of easterly derived fanglomerate (Rock Spring conglomerate) shed from the footwall of the Cyclopic fault and possibly from Garnet Mountain along the western margin of the Colorado Plateau. Gently tilted ( $<10^\circ$ ) 13–8 Ma strata within the Grand Wash trough and southern White Hills basin suggest that movement on the Grand Wash and related fault zones, as well as development of major hanging-wall half grabens, occurred primarily between ca. 16 and 13 Ma. Furthermore, the distribution of the Snap Point–Nevershine Mesa basalt flow indicates that the Grand Wash Cliffs have changed little since 8.8 Ma.

These relations suggest that the current physiography of the Colorado Plateau–Basin and Range boundary in northwest Arizona began developing ca. 16 Ma and was essentially established by 13 Ma (Faulds et al., 2001b). Thus, most of the structural and topographic demarcation between the two provinces had developed by ca. 13 Ma. The antiquity and abruptness of the Colorado Plateau–Basin and Range boundary in this region, as well as the stratigraphic record in the southern White Hills, suggest that significant headward erosion into the high-standing plateau began in middle Miocene time. Many deep canyons have since been carved into the Colorado Plateau, the most prominent of which is the Grand Canyon of the Colorado River. It is therefore possible that incipient excavation of the western part of the Grand Canyon by an originally small west-flowing stream also began in the middle Miocene (Faulds et al., 2001b).

However, thick middle to upper Miocene evaporite and lacustrine deposits within the Lake Mead and surrounding regions

(e.g., Lucchitta 1966, 1979; Mannion, 1963; Peirce, 1976; Faulds *et al.* 1997) indicate that a long period of internal drainage followed the onset of major extension and preceded integration by the Colorado River and full development of the Grand Canyon. Nevertheless, the widespread distribution of such deposits (Fig. 9) may signify a large influx of groundwater that possibly issued from Paleozoic limestone aquifers on the Colorado Plateau (e.g., Hunt, 1969; Huntoon, 1996, 2000; Crossey *et al.*, 2002) and/or surface waters from developing drainage systems, both of which may have been related to subsequent development of the Colorado River (Faulds *et al.*, 2001b, 2001c). It is noteworthy that the Hualapai Limestone is restricted to areas relatively proximal to the present course of the Colorado River, whereas thick salt deposits characterize some of the surrounding basins (e.g., Hualapai, Overton Arm, Detrital). It therefore seems likely that some kind of precursor to the Colorado River supplied fresh water to lakes in the Lake Mead area and that some of these lakes were bordered by large playas. The large influx of fresh water may have also fed large groundwater systems that discharged in some of the surrounding isolated basins (e.g., Hualapai basin), forming unusually thick salt deposits in their wake.

The northwestward shift of extension into the western Lake Mead region at ca. 13 Ma is noteworthy due to its possible effect on regional base level (Faulds *et al.*, 2001b). Both the 13–9 Ma event in the western Lake Mead region and localized post–9 Ma deformation accentuated the topographic and structural relief between the extensional corridor and Colorado Plateau that had been largely generated in the 16–13 Ma pulse of extension. The most notable post–9 Ma deformation occurred on the Wheeler Ridge fault in the eastern Lake Mead area (Figs. 2 and 8), which accommodated as much as 300 m of post–6 Ma down-to-the-west displacement of the Hualapai Limestone in the Gregg Basin (Lucchitta, 1966; Howard *et al.*, 2000; Wallace *et al.*, 2005). The post–13 Ma tectonism further lowered base-level in the region and probably rejuvenated down-cutting in the Colorado Plateau, thus facilitating excavation of the Grand Canyon and ultimate development of the through-flowing Colorado River.

### Arrival of Colorado River

Several basins in southern Nevada and northwest Arizona record a transition from lacustrine to fluvial deposition between ca. 6 and 4 Ma that marks the arrival of the Colorado River and presumably main phase of excavation of the Grand Canyon (Faulds *et al.*, 2001c, 2002a; House *et al.*, 2005). As previously discussed, the late Miocene landscape in the Lake Mead region was dominated by a series of lakes or wetlands within which the Hualapai Limestone and temporally correlative lacustrine deposits accumulated. The lakes stretched from the mouth of the Grand Canyon in the Grand Wash trough, through the Temple Bar–northern Detrital basin, and westward to the Boulder Basin in the western Lake Mead area. The ca. 11–6 Ma Hualapai Limestone is the youngest deposit formed prior to integration of the Lake Mead region into a through-flowing Colorado River. In the

Gregg Basin, the 4.4 Ma basalt flow at Sandy Point is intercalated in Colorado River gravels. Farther west, a lacustrine limestone just north of Frenchman Mountain rests on the ca. 5.6 Ma Wolverine Creek tephra and interfingers eastward with a gypsum deposit that extends to near the modern Colorado River (Castor and Faulds, 2001). These relations bracket Colorado River inception in the Lake Mead region between ca. 5.6 and 4.4 Ma.

To the south in the Lake Mohave and Laughlin–Bullhead City area, alluvial fans dominated the late Neogene landscape until ca. 5.6 Ma when small lakes formed (House *et al.*, 2005). Near Bullhead City, the 5.6 Ma Wolverine Creek tephra lies directly below a thin limestone. Nearby, younger Colorado River gravels contain the 3.6–4.2 Ma “lower Nomlaki” tephra. Thus, inception of the Colorado River in the Lake Mohave area is bracketed between ca. 5.6 and 4.2 Ma (House *et al.*, 2005), similar to that in the Lake Mead region. Farther south in the Salton Trough region of southern California, the first appearance of Colorado River sand occurred ca. 5.3 Ma (Dorsey *et al.*, 2005, 2007).

These relations indicate relatively rapid, regional inception of the lower Colorado River in the early Pliocene throughout northwest Arizona, southern Nevada, and southern California. The chemistry of late Neogene lakes in this region may hold important clues to the mechanisms of inception and is currently under investigation by Roskowski *et al.* (2007).

## DAY 1. LAS VEGAS TO GRAND WASH TROUGH

### Introduction

Figure 3 shows an overview of the trip route for each day. The trip focuses on the northwest corner of Arizona between Lake Mead on the north and Kingman, Arizona, on the south.

On Day 1, we will drive southeast from Las Vegas directly to the Grand Wash trough in the eastern Lake Mead area, crossing the Colorado River at Hoover Dam on the way. Stratigraphic and structural relations within the Grand Wash trough and Gregg Basin are the focus of Day 1. The Grand Wash trough is a composite, east-tilted half graben in the hanging wall of the Grand Wash fault zone. Flat-lying Paleozoic strata on the Grand Wash Cliffs bound the trough on the east.

After overview stops along U.S. Highway 93 approximately 13 miles south of Hoover Dam and on Grapevine Mesa at Airport Point in the Grand Wash trough, subsequent stops will visit (1) a thick section of conglomerate shed from the steeply tilted Gold Butte block to the west, (2) the Wheeler Ridge normal fault, which is part of the Grand Wash fault system and accommodated tilting of post–5 Ma Colorado River sediments, (3) the 4.4 Ma Sandy Point basalt that interfingers with Colorado River sediments, and (4) the ca. 11–6 Ma Hualapai Limestone, which immediately predates arrival of the Colorado River. The stratigraphy within the Grand Wash trough records the structural and paleogeographic evolution of the region and will therefore facilitate significant discussion of the evolution of both the Colorado Plateau–Basin and Range boundary and the Colorado River.

## En Route Discussion

As we leave Las Vegas, we will travel southeast on U.S. Highway 93/95 and continue along Highway 93 through Boulder City. Highway 93 crosses the Colorado River at Hoover Dam at the head of Black Canyon. Black Canyon contains a thick (>2 km) sequence of moderately to steeply east-tilted early to middle Miocene volcanic rocks (mainly basaltic andesite lavas), which rest directly on Paleoproterozoic basement (Anderson, 1978). Most of the major road-cuts near Hoover Dam, however, are in the 13.9 Ma tuff of Hoover Dam, a dacitic, poorly to moderately welded, ash-flow tuff (Mills, 1994). As we skirt Black Canyon along Highway 93, we traverse through multiple road-cuts of incised late Miocene–Pliocene alluvial fan sediments, which include a few large megabreccia deposits of Proterozoic gneiss and are locally capped by 4.3–5.9 Ma basalt lavas (Feuerbach et al., 1993). These deposits are essentially untilted and overlie east-tilted strata as young as 12.6–11 Ma. Thus, they record a largely post-extensional ca. 11–5 Ma episode of erosion of the Wilson Ridge crystalline terrane and subsequent dissection by the Colorado River and its tributaries.

### Directions to Stop 1-1

Proceed from Las Vegas to Hoover Dam. From Hoover Dam, drive ~12.95 miles south on U.S. Highway 93, then pull off to right at overlook.

### Stop 1-1. Willow Beach Overlook

The Willow Beach overlook provides sweeping views to the west of Black Canyon along the Colorado River and much of the northern Eldorado and northern Black Mountains. The classic early studies of Anderson (1971, 1978) and Anderson et al. (1972) of large-magnitude Miocene extension were conducted in this region. The Colorado River is below, and the Eldorado Mountains lie to the west of the Colorado River. The high ridge to our east is Wilson Ridge, a large horst block dominated by the ca. 13 Ma Wilson Ridge pluton (Larsen and Smith, 1990) in the north and Paleoproterozoic gneisses in the south. Most of the region within view is part of the Lake Mead extensional domain (Spencer and Reynolds, 1989), which is dominated by steeply east-tilted fault blocks bounded by gently to steeply west-dipping normal faults.

Malpais Flattop Mesa is the prominent basalt capped mesa to the southwest.  $^{40}\text{Ar}/^{39}\text{Ar}$  dating of variably tilted volcanic units within an east-tilted half graben along the west flank of Malpais Flattop Mesa brackets major deformation in this area between ca. 15.9 and 11 Ma (Faulds, 1999; Faulds et al., 1999). The gently (~5°) east-tilted basalt lavas that cap Malpais Flattop Mesa have yielded  $^{40}\text{Ar}/^{39}\text{Ar}$  ages of 11.3–11.6 Ma. Thus, the capping basalts on Malpais Flattop Mesa are appreciably older than the 4.3–5.9 Ma basalts that overlie the fanglomerates on the west flank of Wilson Ridge.

**En Route Discussion.** About 3.5 miles south of the Willow Beach overlook, we travel through Housholder Pass, where the highway descends into Detrital Valley and expands to four lanes.

Note the contrast between the subdued, relatively undissected topography of Detrital Valley and the highly dissected Black Canyon area. Seismic reflection profiles indicate that Detrital Valley is bordered on the west by a major steeply east-dipping normal fault (Fig. 2). These profiles also suggest that highly reflective middle crust indicative of synextensional ductile fabrics (e.g., McCarthy et al., 1991) lies at a relatively shallow depth (~5–6 km) beneath this area (Faulds, 1999). Drill holes show that the Detrital basin contains several hundred meters of late Miocene halite and gypsum. As we continue south on Highway 93, Mount Perkins in the central Black Mountains comes into view on the west. Mount Perkins is a steeply west-tilted fault block bounded on its east flank by a major gently east-dipping normal fault. The Mount Perkins block exposes an ~9 km thick crustal section, including parts of a large stratovolcano and rhyolite dome complex (Faulds et al., 1995). The west-tilted Mount Perkins block lies within the Whipple domain (Spencer and Reynolds, 1989), which is dominated by west-tilted fault blocks bounded by east-dipping normal faults. To our west, the Black Mountains accommodation zone separates the east-tilted Lake Mead domain from the west-tilted Whipple domain (Faulds et al., 1990, 2001a).

After we turn east onto the Pearce Ferry Road and pass through Dolan Springs, the highway passes through a broad saddle between the southern White Hills on the north and northern Cerbat Mountains to the south (Fig. 3). A large composite east-tilted half graben comprises the southern White Hills and contains ~3 km of middle to upper Miocene synextensional strata (Price, 1997; Price and Faulds, 1999; Faulds et al., 2001b). Table Mountain Plateau is the prominent basalt-capped mesa to the north and consists of gently east-tilted 8.7 Ma basalt flows. More steeply east-tilted strata form hogback ridges directly west of the Table Mountain Plateau. The southern White Hills basin lies in the hanging wall of the Cyclopic–Cerat Mountains fault (southern part of the South Virgin–White Hills detachment fault) and will be the focus of Day 3 of the field trip.

After passing through the saddle, the Pearce Ferry Road gently descends into the north end of the Hualapai basin before climbing onto Grapevine Mesa in the southernmost part of the Grand Wash trough. As we ascend onto Grapevine Mesa, a large west-protruding promontory of the Colorado Plateau, Garnet Mountain, is on the right, and the south end of the Lost Basin Range lies to the left. Once atop Grapevine Mesa, we travel northward through a thick Joshua tree forest and gradually descend toward Airport Point at the north end of Grapevine Mesa. Directly east of Grapevine Mesa lies the imposing fault-line escarpment of the Grand Wash Cliffs, which consist of very gently (<~3°) north-east-tilted Paleozoic strata in the footwall of the northern Grand Wash fault (Figs. 1, 4, and 5). The Grand Wash Cliffs mark the abrupt western margin of the Colorado Plateau in this region.

### Directions to Stop 1-2

From the Willow Beach overlook (Stop 1-1), continue south on U.S. Highway 93 for 28.8 miles, then turn left onto the Dolan Springs–Pearce Ferry Road. Continue on the Pearce Ferry Road for

43.8 miles, traversing through the town of Dolan Springs (~6.0 miles from the turnoff), north end of the Hualapai basin, and Grapevine Mesa along the way. At 43.8 miles past the turnoff from Highway 93, turn right onto a dirt road and travel 2.8 miles to Airport Point.

### Stop 1-2. Airport Point, Grapevine Mesa, Grand Wash Trough

Airport Point provides a panoramic view of the abrupt transition between the Colorado Plateau and Basin and Range province (Fig. 4), including the Grand Wash Cliffs and mouth of Grand Canyon to the east, steeply tilted fault blocks and Miocene synextensional strata within the Grand Wash trough to the north, and the steeply tilted Gold Butte block to the west. Airport Point lies in the central part of the Grand Wash trough at the north end of Grapevine Mesa, which is a broad plateau capped primarily by the ca. 11–6 Ma Hualapai Limestone. It is noteworthy that the upper relatively flat surface of Grapevine Mesa, developed on the Hualapai Limestone, essentially marks the floor of a lake that immediately predates arrival of the Colorado River.

Early studies in this area include those of Longwell (1936, 1946), Lucchitta (1966, 1972, 1979), and Bohannon (1984). Lucchitta's seminal work, which integrated the stratigraphic and structural framework with the evolution of the Colorado River, produced many concepts that have withstood decades of additional research. More recent work in this area has produced more detailed maps (Howard et al., 2003; Wallace et al., 2005; Brady et al., 2008), constrained the ages of critical units and events with  $^{40}\text{Ar}/^{39}\text{Ar}$  geochronology and geochemical correlations of tephra (i.e., tephrochronology; Faulds et al., 2001b, 2001c; Wallace et al., 2005), refined the depositional environment of the Hualapai Limestone (Wallace, 1999; Faulds et al., 2001c) and other clastic units (Blythe, 2005), and elucidated the structural and paleogeographic evolution of the region (Fryxell et al., 1992; Fitzgerald et al., 1991, 2003; Brady, 1998; Brady et al., 2000; Reiners et al., 2000; Howard et al., 2000, 2008; Faulds et al., 2001b, 2001c).

To our west, the steeply east-tilted Gold Butte block is the northern and widest part of the footwall to the South Virgin–White Hills detachment fault (Figs. 2 and 3). This block has been interpreted as a tilted oblique section through the upper 15–18 km of the crust (Wernicke and Axen, 1988; Fryxell et al., 1992). A series of thermochronologic profiles across the Proterozoic gneiss and granite in the block, using a variety of minerals and techniques, indicate rapid cooling from tectonic unroofing ca. 15 Ma (Fitzgerald et al., 1991; Reiners et al., 2000; Reiners, 2002). The Mesoproterozoic Gold Butte Granite in the block was long ago recognized as the source of large boulders in Miocene debris that spread into the Grand Wash Trough as far as the present-day mouth of the Grand Canyon (Longwell, 1936; Lucchitta, 1966). Debris in middle Miocene deposits at Frenchman Mountain since transported far to the west, near Las Vegas, has also been attributed to sources in the Gold Butte block (Longwell, 1974). Longwell (1936) inferred from the coarseness and wide distribution of sediments derived from the block that the range towered above its surroundings.

To the east of Airport Point, the western margin of the Colorado Plateau is marked by the imposing fault-line escarpment of the Grand Wash Cliffs, which rise ~1.3 km above the Grand Wash trough. Paleozoic strata on the Grand Wash Cliffs are tilted very gently (generally  $<3^\circ$  and commonly  $<1^\circ$ ) to the northeast. This northeast-tilting is inherited from regional uplift to the west and southwest during Laramide time and, in this region, essentially marks the north to northeast flanks of the Kingman arch (e.g., Bohannon, 1984; Peirce, 1985). As a result of this gentle northeast tilting, a series of northwest-trending erosional escarpments developed during early Tertiary time in Paleozoic and Mesozoic strata across the southwestern part of the Colorado Plateau. One prominent escarpment in this region formed at the base of resistant formations of Permian limestone (Toroweap and Kaibab Formations) and is still very conspicuous in the present physiography of the Grand Canyon region.

The west-dipping northern Grand Wash fault lies near the base of the Grand Wash Cliffs but is overlapped by late Miocene strata within the Grand Wash trough (Lucchitta, 1966). Fault blocks in the hanging wall of the northern Grand Wash fault, such as Wheeler Ridge to our north and the Gold Butte block to our west, are tilted steeply eastward ( $>60^\circ$ ), suggesting that the northern Grand Wash fault has a listric geometry. The contrast between the nearly flat-lying Paleozoic strata along the Grand Wash Cliffs and the steeply east-tilted Paleozoic strata on Wheeler Ridge (just 10 km west of the Grand Wash Cliffs), which can be easily seen to the north of Airport Point (Fig. 4), epitomize the abrupt transition between the Colorado Plateau and Basin and Range province in this region. It is noteworthy that the aforementioned, prominent northwest-trending early Tertiary escarpment at the base of the resistant Permian limestones on the Colorado Plateau is also preserved on Wheeler Ridge but has been tilted steeply eastward along with the rest of the fault block (Lucchitta and Young, 1986). Progressive erosional beveling toward the south removed the north- to northeast-tilted Paleozoic strata from most of the northern Colorado River extensional corridor, where Miocene strata generally rest directly on Proterozoic basement.

Significant displacement along the listric, northern Grand Wash fault zone generated the east-tilted composite half of the Grand Wash trough, which filled primarily with middle to upper Miocene sedimentary deposits. Tilt fanning within these sedimentary rocks indicates that the main pulse of extension began prior to ca. 15.3 Ma and ended by ca. 13 Ma; however, the Hualapai Limestone and an overlying 4.4 Ma basalt intercalated in Colorado River sediments are locally tilted and faulted, demonstrating that some extension continued into Pliocene and possibly Quaternary time. It is noteworthy that an 8.8 Ma basalt lava flowed down the Grand Wash Cliffs from the Snap Point area to Nevershine Mesa (Figs. 2 and 3), indicating that the physiography of the Grand Wash Cliffs has changed little since late Miocene time (Faulds et al., 2001b). On subsequent stops, we will view critical parts of the stratigraphic section within the Grand Wash trough and discuss how parts of this section reflect major deformational events and may or may not be related to development of the Colorado River.

**Directions to Stop 1-3**

From Stop 1-2, return to the Pearce Ferry Road and turn right (north). The road descends through a thin veneer of Hualapai Limestone, the underlying sandstone-siltstone facies, and then into a thick section of coarse conglomerate. After 1.5 miles on the Pearce Ferry Road, turn left onto the South Cove Road and travel 0.9 miles to Stop 1-3 (pull off on right shoulder).

**Stop 1-3. Roadcuts in Fanglomerate Facies**

Roadcuts here expose a thick sequence of massive, gently east-dipping, generally matrix-supported conglomerate. The conglomerate contains many large boulders (some >5 m long) of the 1.4 Ga Gold Butte Granite, a megacrystic rapakivi granite derived from the Gold Butte block in the south Virgin Mountains ~6–10 km to the west (Longwell, 1936; Lucchitta, 1966; Lucchitta and Young, 1986; Wallace, 1999; Blythe, 2005). Easterly dips in the 250-m-thick section of conglomerate on the west flank of Grapevine Mesa decrease upward from ~25° to ~5°. Rock avalanche megabreccia deposits are locally intercalated in the conglomerate, especially in the lower part of the section. The conglomerate is roughly bracketed between ca. 15.3 and 11 Ma.

The poor sorting, angularity and size of clasts, both matrix- and clast-supported beds, and intercalated lenses of sandstone suggest that the conglomerate originated as debris-flow and sheetflood deposits on alluvial fans. The conglomerate was deposited in large alluvial fan complexes shed eastward from the Gold Butte block and in some cases filled paleocanyons cut into east-tilted Paleozoic strata (Lucchitta and Young, 1986). These fanglomerates reflect relative uplift of the Gold Butte block and subsidence of the Grand Wash trough, both induced by significant east-tilting in the hanging wall of the northern Grand Wash fault zone and possibly some isostatic rebound of the Gold Butte block, which lies in the footwall of the South Virgin–White Hills detachment fault. Their westerly provenance indicates that no major through-going drainages flowed westward from the Colorado Plateau during this interval (Lucchitta, 1966).

**Directions to Stop 1-4**

Continue to the west on the South Cove Road, descending through the massive conglomerate and passing the Miocene unconformity on the right, where the conglomerate rests in angular unconformity on Paleozoic strata. After 1.2 miles, pull off to right into large parking area.

**Stop 1-4. Wheeler Ridge Fault and Gregg Basin**

We will traverse up the hill to the southeast of the South Cove Road to the Wheeler Ridge fault. The fault trace is marked by steeply (5°–70°) west-dipping flat-irons of the Hualapai Limestone dragged along the fault and juxtaposition of the limestone against the conglomerate that contains clasts of the Gold Butte Granite. The Wheeler Ridge fault bounds the Gregg Basin on the east. The Gregg Basin is a narrow east-tilted half graben that

merges northward with the Grand Wash trough. Our traverse provides an excellent southward view of the Gregg Basin, including a hanging-wall syncline induced by east-tilting of the half graben and west-facing drag along the Wheeler Ridge fault (Fig. 8). The Wheeler Ridge fault accommodated ~300 m of down-to-the-west normal displacement of the ca. 11–6 Ma Hualapai Limestone (Lucchitta and Young, 1986; Wallace et al., 2005), and its hanging wall exhibits an east-facing rollover anticline in the Gregg Basin, affecting Colorado River sediments intercalated with a 4.4 Ma basalt flow at Sandy Point (Howard et al., 2000).

**Directions to Stop 1-5**

Continue 1.5 miles downhill to the west on the South Cove Road, then veer right and travel 0.3 miles to the picnic area for lunch.

**Stop 1-5. Sandy Point Viewpoint**

A short stroll to the west from the picnic area provides a view to the north of the peninsula of Sandy Point, where a 4.41 ± 0.03 Ma basalt flow (Faulds et al., 2001c, from M. Kunk, 1998, written commun.) is intercalated in Colorado River sediments (Fig. 14). This basalt flow provides an important age constraint on the inception of the Colorado River in the Lake Mead area. The Hualapai Limestone, which predates arrival of the Colorado River, is as young as ca. 6 Ma (Spencer et al., 2001). Thus, inception of the Colorado River in the eastern Lake Mead area is constrained between ca. 6 and 4.4 Ma. The sands and rounded gravels in the picnic area are Colorado River sediments and partly correlate with the Chemehuevi Formation of Longwell (1936, 1946).

Across Lake Mead on the west side of Gregg Basin, the prominent Jumbo Pass wind gap between the Virgin Mountains (to the north) and the Hiller Mountains (to the south) contains rounded river pebbles recording an abandoned high-level paleovalley of the Colorado River across the Gold Butte–Hiller Mountains–White Hills massif (Howard et al., 2003). The Jumbo Pass area may have been a major late Miocene pathway for debris transported from the Gold Butte block toward the Grand Wash trough, as suggested by coarse-grained upper Miocene fanglomerate exposures near and east of the Pass.

**Directions to Stop 1-6**

Return to Pearce Ferry Road by driving 3.8 miles east on South Cove Road. Turn right (south) toward Meadview onto Pearce Ferry Road and continue south 8.9 miles, then pull off to right to optional stop at Gregg Basin overlook.

**Stop 1-6. Gregg Basin Overlook (Optional)**

This overlook lies along the western rim of Grapevine Mesa and therefore provides excellent views to the west of Gregg Basin, the Gold Butte block, Virgin River Canyon along the Colorado River (filled by Lake Mead), and in the distance the Temple Bar–Detrital basin area. The Virgin River Canyon is one of

three places where the Colorado River cut through the large Gold Butte tilt block. Whether the Gregg Basin–Grand Wash trough and Temple Bar–Detrital basin were connected prior to arrival of the Colorado River will be discussed on Day 2.

In the foreground on the east side of Gregg Basin are two exposures of Proterozoic rock separated by the steeply dipping, poorly exposed Meadview fault, which is marked by a 50–100-m-thick damage zone (Wallace et al., 2005; Swaney, 2005). The easternmost Proterozoic exposure lies beneath the Cambrian nonconformity and has yielded a relatively old apatite fission-track age (ca. 125 Ma; Fitzgerald et al., 2003). The exposure west of the Meadview fault, at the northernmost tip of the Lost Basin Range, yielded a relatively young apatite fission-track age of ca. 15 Ma (Fitzgerald et al., 2003). Based on the different cooling and inferred exhumation histories in these adjacent blocks, the Meadview fault appears to be a relatively underappreciated significant fault in this region.

The Colorado River (and now Lake Mead) exits Gregg Basin westward through narrow Virgin Canyon across the Proterozoic rocks of the footwall block of the South Virgin–White Hills detachment fault. Abandoned paleovalleys containing Colorado River pebbles at Jumbo Pass and also south of Virgin Canyon at Spring Canyon mark former courses of the river across the block. The Hualapai Limestone bridges across the block south of Virgin Canyon and demonstrates that in the late Miocene the Gregg basin merged westward with the northern White Hills basin.

#### **Directions to Stop 1-7**

Continue south on Pearce Ferry Road 0.6 miles, then turn left onto Meadview Boulevard and continue east past stop sign at Meadview Market. After 2.0 miles on Meadview Boulevard, turn right onto Shore Avenue. Travel south 0.1 miles on Shore Avenue, then turn left onto unmarked dirt road (Grapevine Wash Road). Continue 1.1 miles on Grapevine Wash Road to Stop 1-7. Note that as the Grapevine Wash Road is sandy and locally rough, high clearance and four-wheel-drive are advised.

#### **Stop 1-7. Sandstone-Siltstone Facies**

A short walk west of the road brings us to an excellent exposure of the sandstone-siltstone facies (in the rocks of the Grand Wash trough), which exceeds 100 m in thickness. The sandstone-siltstone facies is characterized by alternating beds of pale reddish-brown, moderately sorted, fine- to medium-grained sandstone, siltstone, and mudstone, with subordinate lenses of pebble conglomerate and gypsum. This unit interfingers with both the overlying Hualapai Limestone and underlying fanglomerate facies.

The depositional environment of the sandstone siltstone facies was probably a highly evaporative interior continental playa, as evidenced by the intercalated gypsum, thin bedding, and mudcracks (Wallace et al., 2005). The lack of fluvial textures, such as cross-beds or ripple marks, local abundance of gypsum rinds, interfingering and bordering fanglomerate facies,

and interbedded gypsum appear to rule out any rigorous and/or constant through-going drainage, at least in exposed areas.

The fanglomerate and sandstone-siltstone facies are probably related, but the grayish-brown matrix in the Proterozoic-clast fanglomerate contrasts with the reddish sandstone and siltstone. This suggests that at least two different source areas fed sediment into the Grand Wash trough. The Proterozoic-clast conglomerate was probably derived primarily from the crystalline terranes of the south Virgin Mountains and possibly Lost Basin range, whereas the sandstone-siltstone facies may have been largely derived from nonresistant Pennsylvanian-Permian redbeds (e.g., Hermit and Supai Formations) on the Colorado Plateau and/or to the north of the Grand Wash trough.

The exposed part of the sandstone-siltstone facies within this area is bracketed between ca. 13 and 11 Ma. Nonwelded tuffs in the lower part of the exposed section in the Pearce Ferry area have yielded fission-track ages ranging from  $10.8 \pm 0.8$  to  $11.6 \pm 1.2$  Ma (Bohannon, 1984) and a maximum  $^{40}\text{Ar}/^{39}\text{Ar}$  age on sanidine of  $13.11 \pm 0.08$  Ma, whereas a tephra in the upper part of the section near Airport Point geochemically correlates with a  $10.94 \pm 0.03$  Ma tuff (Wallace et al., 2005).

#### **Directions to Stop 1-8**

Continue north on Grapevine Wash road and keep left past corral at 0.3 miles. Continue north another 1.3 miles past corral to Stop 1-8.

#### **Stop 1-8. Fanning dips in Hualapai Limestone**

Brief stop in wash to view fanning west-dipping beds in Hualapai Limestone. Dips decrease appreciably up-section in the limestone, and several beds onlap and pinch out against more steeply dipping beds (Fig. 15). These relations indicate that some extension coincided with deposition of the 11–6 Ma Hualapai Limestone.

#### **Directions to Stop 1-9**

Continue north on Grapevine Wash Road 3.0 miles to Stop 1-9. Road will descend into the 200–300 m deep Grapevine Canyon and through much of the 300-m-thick Hualapai Limestone.

#### **Stop 1-9. Hualapai Limestone and 10.94 Ma Tephra**

At this stop, a distinctive light gray tephra is interbedded in the lowermost part of the Hualapai Limestone and is well exposed in a conspicuous enclave and bench on the lower east side of the canyon (Fig. 16) only a few meters east of the road. This tephra geochemically correlates with a  $10.94 \pm 0.03$  tuff derived from the Bruneau-Jarbridge volcanic field in southernmost Idaho (M. Perkins, 1998, written commun.) and has also yielded an  $11.08 \pm 0.27$  Ma  $^{40}\text{Ar}/^{39}\text{Ar}$  date on fine-grained sanidine (Faulds et al., 2001c; Wallace et al., 2005). As such, it provides an excellent older age constraint for the Hualapai Limestone. A tephra within the upper part of the limestone on Grapevine Mesa yielded a poorly defined  $^{40}\text{Ar}/^{39}\text{Ar}$  age of  $7.43 \pm 0.22$  Ma, which should be con-

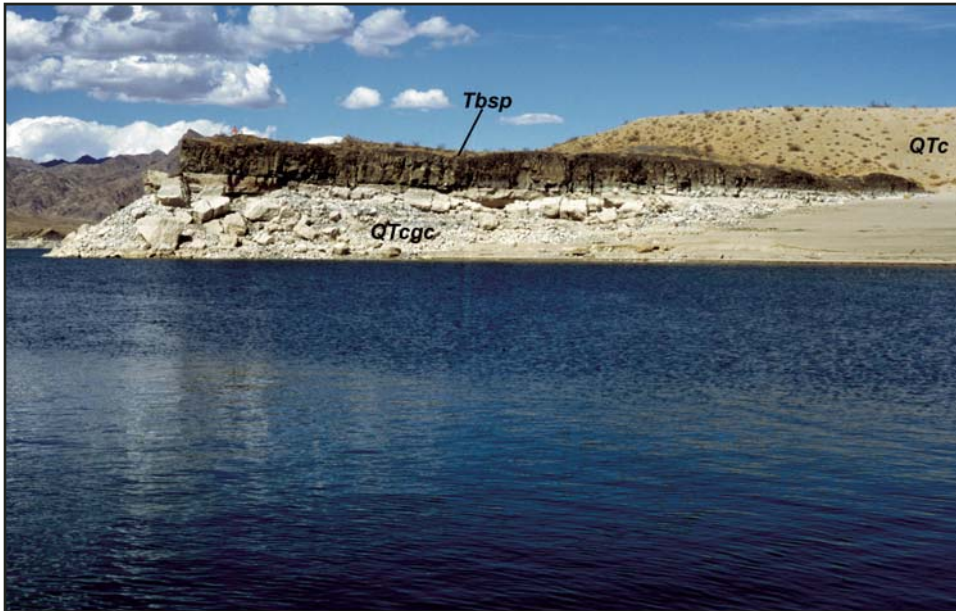


Figure 14. Looking northeast at 4.4 Ma basalt of Sandy Point (Tbsp), which is intercalated in Colorado River sediments (QTc and QTcgc).



Figure 15. View north of growth-fault sequence in Hualapai Limestone in Grapevine Wash. West tilts decrease up section from  $\sim 25^\circ$  to subhorizontal in this area. Note onlap of gently dipping beds against more steeply tilted layers. This deformation has been attributed to minor normal faulting (Wallace et al., 2005).



Figure 16. View north of ca. 11 Ma tephra near base of the Hualapai Limestone in Grapevine Canyon. Black arrows point to  $\sim 1\text{--}2$  m light gray tephra beneath ledge of limestone.

sidered a maximum eruptive age (M. Heizler, 1999, written commun.). A tephra interbedded within the upper part of the Hualapai Limestone in the Temple Bar area ~25 km to the west of the Grand Wash trough yielded an  $^{40}\text{Ar}/^{39}\text{Ar}$  age of 6.0 Ma (Spencer et al., 2001), which has been widely used as a younger age constraint on the Limestone in the Lake Mead area. The Hualapai Limestone in the Grand Wash trough may therefore be as young as ca. 6 Ma.

In both the Gregg Basin and Grapevine Wash area of the Grand Wash trough (Figs. 2 and 5), the Hualapai Limestone appears to form large lenticular wedge-shaped deposits that thicken eastward toward the deeper parts of the half grabens and onlap older units along the western margins of the basins. In the Grapevine Wash area, the limestone consists of a thick (~300 m) section of wavy laminated, vuggy pelleted packstone, wackestone, and calcareous mudstone, with rare siltstone laminations (Wallace, 1999). Petrographic analysis indicates that the limestone is dominantly pelmicrite and rarely contains fossils (Wallace, 1999).

In contrast to the interpretation of Blair and Armstrong (1979), detailed analysis of the limestone revealed no evidence of a marine or estuarine setting (Wallace, 1999; Faulds et al., 2001c). Fossils include only ostracodes, green algae (including charophytes), algal mats, oncolites, and stromatolites in a typically pelleted micrite substrate. None of the fossils are diagnostically marine (e.g., Heckel, 1972). Ostracodes are highly tolerant organisms that can live in extreme conditions that include fresh to hypersaline, clear to sediment-loaded water. Blue-green and green algae can also live in several environments but are constrained to the photic zone. However, charophytes need clear, fresh water to survive (Heckel, 1972). Furthermore, locally abundant flowstone indicates a constant source of fresh water super-saturated in calcium carbonate, either issuing from springs or perennial streams. In addition, low  $\delta^{18}\text{O}$  values and highly variable  $\delta^{13}\text{C}$  characterize the Hualapai Limestone (Wallace, 1999), both of which are indicative of a nonmarine setting (e.g., Talbot and Kelts, 1990). The composition and isotopic characteristics of the Hualapai Limestone indicate deposition in one or more restricted warm, shallow, and quiet lakes fed by a relatively continuous source of fresh water in an evaporative climate (Wallace, 1999; Faulds et al., 2001c). In order to stay fresh, the lake or lakes probably had an outlet.

## DAY 2. KINGMAN TO NORTHERN WHITE HILLS

### Introduction

On Day 2, we will focus on the South Virgin–White Hills detachment fault, synextensional sedimentary deposits in east-tilted half grabens (northern White Hills basin) in the hanging wall of the detachment, and upper Miocene paleovalleys connecting the Grand Wash trough–Gregg Basin with the northern White Hills basin and Temple Bar–Detrital basins farther west. Although the Grand Wash fault clearly marks the structural and physiographic boundary between the Colorado Plateau and Basin and Range province in this region, the South Virgin–White Hills detachment fault is considered the most significant normal fault in

the eastern part of the Lake Mead domain, as it accommodated as much as 17 km of normal displacement along the west flank of the Gold Butte block directly north of Lake Mead (Brady et al., 2000), about three times the maximum displacement on the Grand Wash fault, and it accommodated >5 km of displacement in the southern White Hills. Thus, the South Virgin–White Hills detachment fault accommodated large-magnitude extension within <30 km of the western margin of the Colorado Plateau and clearly records a progressive westward increase in strain across this region.

### Directions to Stop 2-1

From the hotel in Kingman, drive north on Andy Devine Boulevard 0.4 miles north to Interstate 40 (I-40). Go west on I-40 1.0 miles and take the Stockton Hill exit. Travel north on Stockton Hill Road 49.5 miles to its end at the intersection with the Pearce Ferry Road. Turn right onto the Pearce Ferry Road and travel 0.4 miles to the east, then turn left (north) onto the Gregg's Hideout Road. After 3.1 miles, the Gregg's Hideout Road jogs to the west, so veer to the left, travel 0.9 miles west, then veer back to the right, heading north again on the Gregg's Hideout Road. Then, continue north 7.3 miles on the Gregg's Hideout Road, before turning left toward Temple Bar. Go west on the Temple Bar road 6.8 miles, then turn right (north) into Salt Spring Wash. Travel north in Salt Springs Wash 1.7 miles to Stop 2-1 (Fig. 10).

### Stop 2-1. Salt Spring Detachment, Part of the South Virgin–White Hills Detachment Fault

Walk east a few hundred meters up small wash. Note chlorite cataclasite (or breccia) with subhorizontal fabric on wash walls. This is part of the damage zone associated with the detachment. Note its thickness (as you walk up wash) and the gently west-dipping mesoscopic faults or shear bands. Kinematic indicators, including asymmetric boudins, sigmoidal foliations, and shear bands within the cataclasite record top-west shear sense, consistent with the east-northeast dip of upper-plate strata. In addition, highly altered (to orange color) and offset basalt dikes corroborate the top-west shear sense. At the top of the wash, a white tuff rests directly on the fault surface. We can debate whether the tuff was deposited on the fault surface or is downfaulted against it. In view of the fact that a 15.2 Ma east-tilted tuff is present in the hanging wall just west of Salt Spring Wash, we prefer the latter interpretation. Within this vicinity, small exposures of a brown microcrystalline rock mark the detachment fault proper. This rock is an ultracataclasite, and we interpret it as analogous to the well-known and thicker “microbreccia ledge” of higher-displacement detachments.

Structurally below the detachment surface proper, a zone of greenschist-grade retrogression is present that ranges in thickness from 50 to more than 150 m. This retrogression is superimposed on regional, granulite-facies Proterozoic metamorphism (e.g., Volborth, 1962; Duebendorfer et al., 2001). Although variable, foliation in the footwall of the South Virgin–White Hills detachment generally dips less than 30° to the west in contrast to the generally steep to subvertical dips that characterize crystalline

rocks throughout northwestern Arizona (Blacet, 1975; Duebendorfer et al., 2001). The coincidence of gently dipping foliation with pervasive (Miocene?) retrogression of rocks in the lower plate suggests that tilting of the footwall accompanied motion along the South Virgin–White Hills detachment fault.

#### **Directions to Stop 2-2**

Travel back to the south 0.1 miles in Salt Springs Wash.

#### **Stop 2-2. Middle Miocene Synextensional Deposits**

Take a short traverse through east-dipping conglomerate, sedimentary breccia (all crystalline clasts), and well-bedded sandstone toward a prominent outcrop of white pegmatite. The conglomerates and sedimentary breccias are interpreted as distal debris flow deposits because of their typically nonbedded, matrix-supported character. At the top of a small hill, an outcrop of highly and pervasively shattered pegmatite marks the base of a massive megabreccia sheet that ranges in thickness from 50 to more than 200 m and can be followed along strike for more than 1000 m. This sheet is overlain by an ash-flow tuff dated at 15.2 Ma ( $^{40}\text{Ar}/^{39}\text{Ar}$ , sanidine, Duebendorfer and Sharp, 1998; Fig. 17). The megabreccia deposits within this lower sequence of the hanging-wall section are clearly interbedded with stratified sedimentary rocks and are thus not fractured crystalline rocks of the lower plate that have been somehow infaulted with hanging-wall rocks. The megabreccias exhibit both crackle and jigsaw breccia textures (Yarnold and Lombard, 1989) and are interpreted as catastrophic rock avalanche deposits which are commonly associated with topographic relief generated by active faults (e.g., Yarnold and Lombard, 1989; Topping, 1993), in this case, the South Virgin–White Hills detachment fault.

#### **Directions to Stop 2-3**

Travel back in Salt Springs Wash to the north 0.9 miles.

#### **Stop 2-3. Spectacular Exposure of Huge Megabreccia Deposit**

Fault-like rocks in a megabreccia deposit are exposed on the ridge west of the wash. An underlying debris flow deposit is evident at the level of the wash.

#### **Directions to Stop 2-4**

Travel south back uphill in Salt Springs Wash 1.5 miles, past road from Greggs Hideout, and continue another 3.0 miles.

#### **Stop 2-4. Fault Cataclasite on the Salt Springs Detachment**

An iron-stained ledge of cataclasite dips gently north here over a footwall of retrograded gneiss in the footwall of the South Virgin–White Hills detachment fault. The footwall here in the Golden Rule Peak area is part of a prominent westward salient, and coincides with a steep gravity gradient over the footwall rocks. The poorly exposed hanging-wall rocks in this area include granite and gneiss as well as unconformably overlying Miocene sedimentary deposits of megabreccia and fanglomerate.

#### **Directions to Stop 2-5**

Return northward 3.0 miles, passing en route a dipping white ash-fall tuff that is interbedded with fanglomerate and is correlated by Andrei Sarna-Wojcicki with a 12.0 Ma tephra. Turn back to the right on the road toward Greggs Hideout. Proceed 6 miles, partly along the South Virgin–White Hills detachment fault boundary between the dipping section of fanglomerate and 12 Ma tuff juxtaposed against Proterozoic gneiss in the

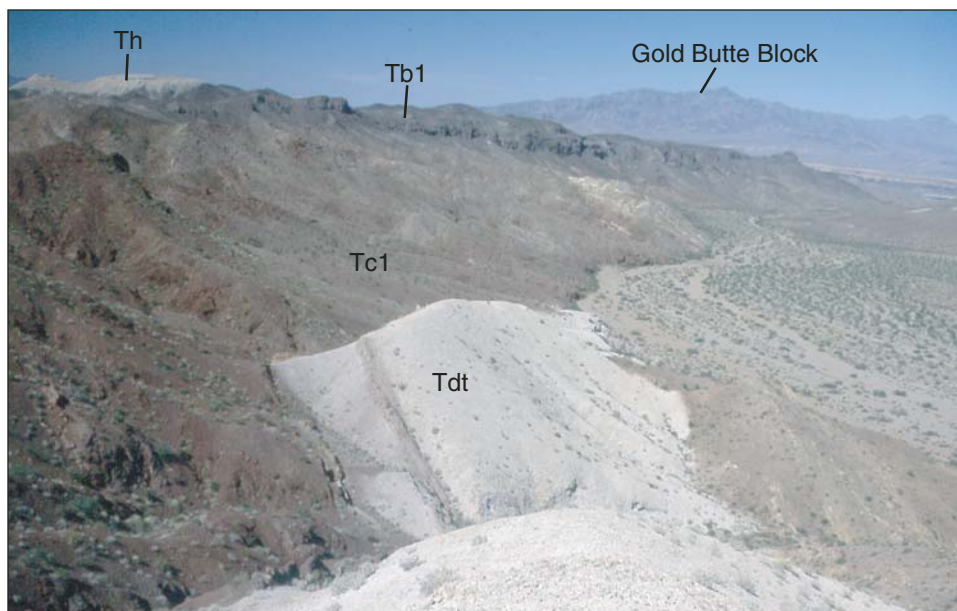


Figure 17. View to north of Salt Spring Wash. The Gold Butte block, which lies in the lower plate of the South Virgin–White Hills detachment fault, is on the horizon (right distance). White unit in the foreground is a poorly welded ash-flow tuff (Tdt) dated at 15.2 Ma that is interbedded with megabreccia and debris-flow deposits (Tc1) in the upper plate of the South Virgin–White Hills detachment. This tuff probably correlates with the tuff of Mt. Davis (e.g., Faulds et al., 2002b). These rocks are tilted 50–60° east and are unconformably overlain by a 20° north-east-dipping, 14.6 Ma basalt flow (Tb1, dark cap rock in the middle distance). White unit at upper left is the flat-lying, 11–6 Ma Hualapai Limestone (Th).

footwall of the Salt Spring detachment, and then through the footwall gneisses

### Stop 2-5. Deposits of Hualapai Wash

Walk southwest up short gully to examine a sequence of sandstone and siltstone that underlies cliff-forming cemented fanglomerate (Fig. 18). This sequence may record the initial entry of the Colorado River onto a basin floored by Hualapai Limestone before the river began incising into the limestone (Howard and Bohannon, 2001). For many miles the sequence can be traced concordantly overlying the gently east-dipping Hualapai Limestone and is tilted gently east with the limestone toward the Wheeler Ridge fault system. The fine-grained deposits in places contain rare rounded pebbles of chert, limestone, and quartzite, clasts typical of Colorado River deposits. Note clayballs and other structures in the sandstone. No other Colorado River fluvial deposits in the Basin and Range province are as high in elevation as these remnants, >700 m.

#### Directions to Stop 2-6

Continue eastward 0.8 miles to Greggs Hideout Road and turn left. Proceed north 7.2 miles to Greggs Hideout on Lake Mead, passing outcrops of Hualapai Limestone en route that are unconformable on the gneisses in the footwall block of the South Virgin–White Hills detachment fault.

### Stop 2-6. South Virgin–White Hills Detachment Fault at Greggs Hideout

The South Virgin–White Hills detachment fault is well exposed at Greggs Hideout as a gouge zone dipping 37° under fanglomerate in the hanging wall (Fig. 19). The fanglomerate in the hanging wall is near-horizontal except within 100 m of the fault, where it bends to 38° dip into the fault and is broken by small-displacement faults. Breccia of Proterozoic rock in the footwall may be either tectonic breccia along the fault zone, or a sliver of megabreccia deposit. Younger horizontal fanglomerate that forms bluffs high to the east overlaps the fault and its footwall. The large boulders in the upper fanglomerate consist of granite closely resembling the Gold Butte Granite. Two kilometers north of here the fault dips more gently over gneiss and granite in the footwall.

#### Directions to Stop 2-7

Return back eastward on the Greggs Hideout Road 1.4 miles to the top of a grade.

### Stop 2-7. Colorado River Paleochannel and Views of Hualapai Limestone Paleovalley Fill on the Footwall Block

Walk northward across lags of rounded river gravel and up a hill underlain by undeformed upper Miocene fanglomerate for views. This site is just south of where the Colorado River crosses the footwall block in Virgin Canyon, and the high-level rounded gravels encountered record an abandoned Pliocene paleovalley of

the river. The northern White Hills basin to the west and southwest is capped by the upper Miocene Hualapai Limestone. The Hualapai Limestone and underlying fanglomerate, which here bridge across the footwall block and connect the White Hills and Greggs basins, postdate the latest motion on the South Virgin–White Hills detachment fault. From this vantage, a paleovalley fill of the Hualapai Limestone is easy to view as inset into the gneisses of the footwall (Fig. 20). The Hualapai Limestone to the east dips gently eastward in the rollover fold against the Wheeler Ridge fault. Spring Canyon, north of the limestone paleovalley fill, contains rubble derived from the limestone that suggests the canyon was also once occupied by the limestone. Rounded river gravels overlying that rubble indicate that the paleovalley was then occupied by a Pliocene course of the Colorado River. The paleovalley and its remnant strings of rubble and river gravels now slopes gently eastward, which suggest that it was back tilted and its drainage direction reversed during development of the rollover fold toward the Wheeler Ridge fault system.

## DAY 3. KINGMAN TO SOUTHERN WHITE HILLS (THEN RETURN TO LAS VEGAS)

### Introduction

Day 3 will involve an overview of the Hualapai basin and an east to west traverse across the southern White Hills basin. The Hualapai basin contains a 2.5-km-thick, middle to late Miocene halite deposit, one of the thickest known nonmarine salt deposits (Faulds et al., 1997). However, because the Hualapai basin is a closed depression that has not been dissected by tributaries to the Colorado River, synextensional deposits are not exposed. Interpretations for this basin are therefore based on geophysical and well data. Two stops will provide an overview of the Hualapai basin and neighboring northern Cerbat Mountains. We will then cross the west-dipping Cerbat Mountains–Cyclopic fault (southern leg of the South Virgin–White Hills detachment fault) and enter into the southern White Hills basin, where several stops will facilitate discussion of the timing of extension and paleogeographic evolution of the region. The conglomerate of Rock Spring dominates the eastern subbasin of the southern White Hills and records significant erosion of the footwall of the South Virgin–White Hills detachment fault and possibly the western margin of the Colorado Plateau. It will therefore be the focus of several stops.

### En Route Discussion

The eastern part of Kingman resides near the southwestern margin of the Hualapai basin. As we leave Kingman and travel north on the Stockton Hill Road, the Hualapai basin will open up to the east (on our right) and the Cerbat Mountains will dominate to the west. The southern Grand Wash fault bounds the Hualapai basin on the east. The Grand Wash Cliffs and Colorado Plateau lie in the footwall of the southern Grand Wash fault. The western margin of the Colorado Plateau is more highly dissected east of



Figure 18. Stop 2-5. Cliff-forming cemented fanglomerate consistently overlies the deposits of Hualapai Wash, which consist of sandstone, siltstone, claystone, and rare rounded pebbles of limestone, chert, and quartzite. The deposits of Hualapai Wash may record the initial entry of the Colorado River into the Basin and Range province. The deposits of Hualapai Wash and the overlying cemented fanglomerate can be traced for many kilometers northward toward Gregg Basin, everywhere concordantly overlying the folded Hualapai Limestone. The deposits of Hualapai Wash therefore were deposited on the uppermost Miocene basin-filling sequence. Younger Colorado River deposits are inset into Hualapai Limestone and record incision resulting from exterior drainage and lowered base levels.



Figure 19. Detachment fault at Gregg's Hideout (Stop 2-6), marked by black arrow. Foliated gouge separates a hanging wall of internally faulted Miocene fanglomerate from a footwall of breccia, consisting primarily of Proterozoic rock.

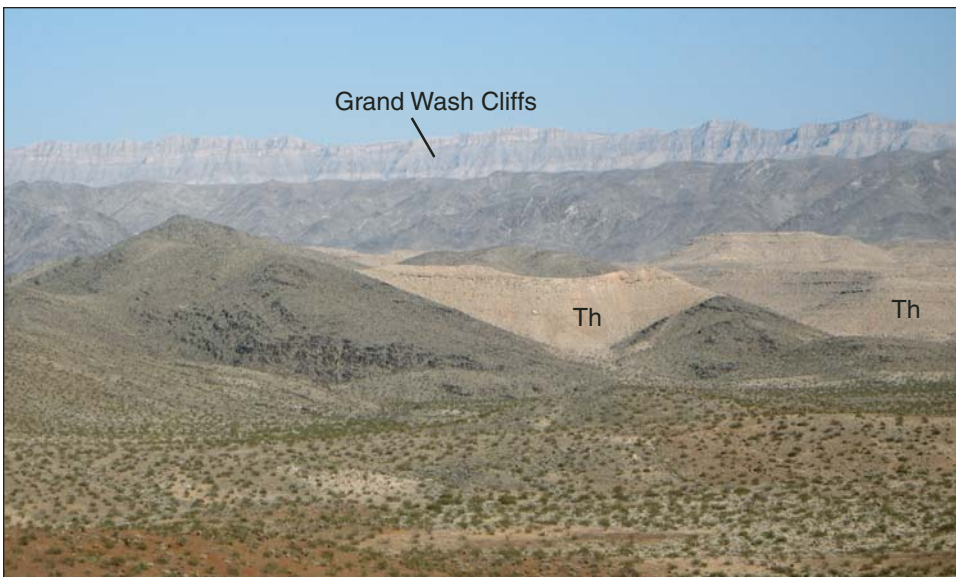


Figure 20. View eastward from Stop 2-7 at light-toned Hualapai Limestone (Th) filling paleotopography cut into dark Proterozoic gneiss in the northern White Hills. The limestone and local underlying upper Miocene conglomerate (red slopes in foreground) here bridge across a low part of the block that forms the footwall of the South Virgin–White Hills detachment fault. The sediments thus record a time when these two basins filled to the point of merging, and drainage basins became more integrated. A younger paleovalley of the Pliocene Colorado River followed a nearby path.

the Hualapai basin than it is to the north directly east of the Grand Wash trough. This morphologic difference probably results from more widespread exposure of less resistant Proterozoic rocks to the east of the Hualapai basin in contrast to the highly resistant Cambrian through Mississippian carbonates that lie directly east of the Grand Wash trough. The aforementioned gentle regional northeast tilt of strata, inherited from early Tertiary time, accounts for the southward trend toward older exposed strata. To our west, the Cerbat Mountains are primarily composed of Paleoproterozoic gneiss and granite (Duebendorfer et al., 2001) but do contain scattered exposures of the basal part of the Tertiary section, especially on the north, east, and southern flanks, as discussed at Stop 3-1. Several gently east-dipping cuestas, capped by resistant volcanic units near or at the base of the Miocene section, grace the east slopes of the Cerbat Mountains and will be quite conspicuous along our route.

#### **Directions to Stop 3-1**

From the hotel in Kingman, drive north on Andy Devine Boulevard 0.4 miles to I-40. Go west 1.0 miles on I-40 and take the Stockton Hill exit. Travel north on Stockton Hill Road 34.3 miles to Stop 3-1.

#### **Stop 3-1. Overview of Northern Cerbat Mountains**

The Cerbat Mountains are the upthrown western part of the east-tilted fault block that forms the Hualapai basin. Miocene strata within the Cerbat Mountains rest nonconformably on Paleoproterozoic gneiss. The base of the Miocene section is well exposed in the high rugged ridges to our west and consists, in ascending order, of an ~10 m thick basal arkosic conglomerate, thin sequence of ca. 20 Ma basalt flows, and ~250 m of matrix-supported, volcanoclastic conglomerate and intercalated trachybasaltic andesite to trachydacite lavas. A flow near the top of this sequence yielded an  $^{40}\text{Ar}/^{39}\text{Ar}$  age of 18.3 Ma. The volcanoclastic conglomerate comprises the bulk of the high jagged ridges, as well as the prominent pinnacles that dominate the skyline east of the town of Dolan Springs. These ridges contain some of the best exposures of the base of the Miocene section in the northern Colorado River extensional corridor. The 18.5 Ma Peach Springs Tuff, which is well-exposed near Kingman, pinches out northward across the Cerbat Mountains and has not been observed in the northern part of the range. All strata in the northern Cerbat Mountains dip gently east (~15°–22°) and are cut by a series of moderately to steeply west- to southwest-dipping normal faults.

#### **Directions to Stop 3-2**

Continue north on the Stockton Hill Road 7.6 miles. We will climb to the top of small ridge directly west of the road for an overview of the Hualapai basin.

#### **Stop 3-2. Overview of Hualapai Basin and Red Lake Playa**

The Hualapai basin contains one of the thickest known, non-marine halite deposits in a continental rift, a 2.5-km-thick section

of middle to late Miocene salt (Faulds et al., 1997). As evident by Red Lake Playa directly east of the Stockton Hill Road, the Hualapai basin is a closed, internally drained depression. The Gregg Basin to the left drains northward to the Colorado River. A very low saddle separates the Gregg and Hualapai basins. Integration of the Hualapai basin into the Colorado River drainage is probably imminent. The salt deposit within the Hualapai basin is not exposed. Saline groundwater noted by ranchers provided the first evidence of subsurface salt. Oil companies drilled the basin in the 1950s in hopes of finding hydrocarbons trapped by a presumed subsurface salt dome. Subsequently, the salt was studied as a potential natural gas repository by the El Paso Natural Gas Company (F.E.R.C., 1982), who drilled additional deep holes in the basin and acquired seismic reflection profiles.

Seismic reflection and drill-hole data indicate that the little-deformed, unexposed halite is 2.5-km-thick in the central part of the basin, approaches ~200 km<sup>3</sup> in volume, and has a three-dimensional lenticular-wedge geometry (Fig. 13). An age of 13–8 Ma is suggested for the salt because it lies in the upper, more gently tilted part of a growth-fault sequence, and extension in the region is bracketed between ca. 16 and 8 Ma. The texture and bromine content of the halite, dominance of halite, and S and O isotopic values of intercalated and capping anhydrite indicate that halite deposition took place in an intracontinental playa that accommodated regional groundwater discharge. Several events conspired to produce this unusually thick salt deposit, including regional aridity, a broad catchment basin with a closed drainage network, ample supplies of Na<sup>+</sup> and Cl<sup>-</sup>, and rapidly developing accommodation space within the basin (Faulds et al., 1997). Large evaporite bodies of probable nonmarine origin are common in many of the basins of southern and central Arizona (Peirce, 1976).

The ridges to the west of the road consist of Paleoproterozoic gneiss capped by ca. 18 Ma basaltic trachyandesite flows. These ca. 18 Ma basaltic andesite lavas may correlate with a southwestward thickening sequence of lower Miocene lavas of similar age and composition in the Iron Mountain and Garnet Mountain areas (e.g., 17.4 Ma—K/Ar age reported in Lucchitta and Young 1986; Wenrich et al., 1996) along the western margin of the Colorado Plateau.

#### **Directions to Stop 3-3**

Continue north 7.6 miles on the Stockton Hill Road, then turn left onto the Pearce Ferry Road. Travel 4.6 miles on the Pearce Ferry Road and pull off to the left into a gravelly parking area at the foot of a small hill. We will take a short traverse to the top of this hill.

#### **Stop 3-3. Cerbat Mountains Fault**

A short walk will take us to the trace of the Cerbat Mountains fault, which is marked by the contact between 8.7 Ma olivine basalt on the west and Paleoproterozoic gneiss on the east. The Cerbat Mountains fault bounds the southern White Hills basin on the southeast and strikes north-northeast through the saddle

between the southern White Hills and northern Cerbat Mountains. In the footwall of the fault to our east, ca. 18 Ma mafic lavas at the base of the Miocene section cap Paleoproterozoic gneiss, whereas in the hanging to the west, the 8.7 Ma basalts of the Table Mountain Plateau cap a 3-km-thick Miocene section in the southern White Hills basin. The offset of the early Miocene nonconformity between the Table Mountain Plateau area and northern Cerbat Mountains suggests ~4–6 km of normal separation along the northern part of the Cerbat Mountains fault (Fig. 11B). The Cerbat Mountains fault probably dips moderately west in its upper part but has an overall listric geometry, as evidenced by significantly greater tilting of the hanging wall, as compared to the footwall (e.g., as much as 50° in the Table Mountain Plateau area versus ~20° in the northern Cerbat Mountains). A Proterozoic gneiss in the footwall of the Cerbat Mountains fault yielded an apatite fission-track age of ca. 73 Ma, whereas all crystalline rocks in the footwall of the South Virgin–White Hills detachment fault to the north yield apatite fission-track ages of <20 Ma.

The Cerbat Mountain fault merges with the Cyclopic fault (e.g., Blacet, 1975; Myers et al., 1986) directly west of Table Mountain Plateau (Figs. 3 and 11A). Collectively, the two faults define a three-dimensional, scoop-shaped geometry of the southern White Hills basin (Fig. 11). There is no evidence that one fault accommodated offset of the other. It is therefore likely that the Cerbat Mountains fault represents a southern continuation of both the Cyclopic fault and South Virgin–White Hills detachment fault.

The overall length of this fault system from the Gold Butte block on the north to the southern Cerbat Mountains on the south is at least 140 km (Fig. 2). A northward increase in both the breadth and metamorphic grade of the footwall crystalline terrane and a corresponding change in fault rocks from cataclites to mylonites indicate a significant northward increase in displacement on the South Virgin–White Hills detachment fault between the southern White Hills and Gold Butte block (Duebendorfer and Sharp, 1998). In the South Virgin Mountains, the Lakeside Mine segment of the South Virgin–White Hills detachment may have accommodated as much as 17 km of normal displacement (Brady et al., 2000). North of the southern White Hills, this fault zone accommodates the greatest amount of normal displacement within the Lake Mead region. To the south of the southern White Hills, this fault zone essentially borders the eastern edge of the highly extended extensional corridor, as it separates the gently tilted Cerbat Mountain block from highly extended terrane in the Black Mountains. This fault zone is clearly one of the most significant structures in the northern Colorado River extensional corridor.

#### **Directions to Stop 3-4**

Cross Pearce Ferry Road obliquely and turn right onto dirt road, marked by a stop sign at the intersection with the highway (<0.1 miles from Stop 3-3). Travel west on dirt road and veer right around corral after 0.6 miles. Continue 1.6 miles on dirt road to Stop 3-4.

#### **Stop 3-4. View of Faulted 8.7 Ma Basalts**

This stop provides a good view to the south of the gently (~5°–10°) east-tilted 8.7 Ma basalts that cap the Table Mountain Plateau, which are as much as ~250 m thick. The basalts are cut by several west-dipping normal faults and the Cerbat Mountains fault, indicating that minor extension continued to at least ca. 8 Ma. It is possible that the faults cutting the basalt were active contemporaneously with the Wheeler Ridge fault and Lost Basin Range faults to the east (i.e., since 4.4 Ma). The 8.7 Ma basalts overlie the conglomerate of Rock Spring, with little if any angular discordance between the conglomerate and basalts. Other documented lavas of this age in the region cap Callville Mesa in the western Lake Mead area (Feuerbach et al., 1993) and Snap Point along the northern Grand Wash Cliffs on the westernmost margin of the Colorado Plateau (Fig. 2; Faulds et al., 2001b).

The basalts of Table Mountain Plateau probably filled paleochannels cut into the underlying conglomerate of Rock Spring and appear to have pooled in the lowermost part of the southern White Hills basin. They were subsequently tilted eastward, probably in response to movement along the Cerbat Mountains fault. Owing to the highly resistant basalts, the present topography at Table Mountain Plateau (Fig. 12) is clearly inverted from that in late Miocene time.

#### **Directions to Stop 3-5**

As we make our way to the west in the southern White Hills basin between Stops 3-5 and 3-6, we will traverse down-section through the synextensional ca. 16.7–8.7 Ma conglomerate of Rock Spring, with numerous small road cuts exposing the basement-clast conglomerate. It is important to note that this area is currently under development; the network of roads may change significantly with further development.

From Stop 3-5, continue on dirt road 0.6 miles to the north and turn left (west) at major cross road. After 1.0 miles, go straight at oblique cross road, then continue for another 2.3 miles and keep right at Y-intersection. After another 0.9 miles, keep right again after another Y-intersection, then continue 0.6 miles to Stop 3-6, located in a small pass at the crest of the White Hills, where recent excavations have left a large parking area. Prepare for a short hike.

#### **Stop 3-5. Conglomerate of Rock Spring**

The recent excavations at the pass have resulted in a superbly exposed knob of the Rock Spring conglomerate, which still existed during planning of this field trip in September 2007. The matrix supported texture, large clasts of megacrystic Proterozoic granite, and moderate east dips are readily visible in the exposure (Fig. 21). Intercalated in the conglomerate are lenses of basaltic andesite lava and tuff, including the 15.2 Ma tuff of Bridge Spring (cf. Faulds et al., 2002b). Clasts of Proterozoic gneiss and granite dominate the conglomerate of Rock Spring and were largely derived from the footwall of the South Virgin–White Hills



Figure 21. Conglomerate of Rock Spring. View looking south at poorly sorted, matrix-supported conglomerate of Rock Spring, containing abundant clasts of Paleoproterozoic megacrystic granite. Large boulder of megacrystic granite at top of mound is ~5 m long. White dashed lines denote faint bedding, which dips moderately east. Black arrow points to relatively distinct bedding plane. Small white oval surrounds 40-cm-long rock hammer.

detachment fault (Cyclopic and Cerbat Mountains segments). Abundant clasts of Proterozoic megacrystic granite throughout the ca. 16.7–8.7 Ma section of conglomerate further suggest that the Garnet Mountain area along the western margin of the Colorado Plateau may have been a source for some of the detritus. These relations indicate significant headward erosion into the footwall of the South Virgin–White Hills detachment fault and possibly the western margin of the Colorado Plateau by west-flowing drainages as early as middle Miocene time.

A short ~0.5 mile walk to the south will bring us to a nice vantage point, with panoramic views of the southern White Hills. Appreciable tilt fanning can be observed to the south, whereby the 15.2 Ma tuff of Bridge Spring is tilted ~35° east in a prominent hogback and the capping 8.7 Ma basalts at Table Mountain Plateau dip ~5° east. Dips in the conglomerate in this area, slightly down section of the tuff of Bridge Spring, are ~55°. Tilt fanning within the southern White Hills indicates that major east-west extension occurred from ca. 16.7–8 Ma. As we traverse through exposures of the Rock Spring conglomerate, note the abundant clasts of garnet-bearing gneiss and megacrystic granite, as well as a thin basaltic andesite flow. To the north, the prominent peak of Senator Mountain can be seen. Senator Mountain is capped by ca. 9.9 Ma basalt flows that slope gently west but overlie the gently east-tilted Rock Spring conglomerate. A north-striking basalt dike directly east of Senator Mountain probably fed these flows, which flowed westward in a paleochannel, which has now been inverted due to the resistant basalts.

#### **Directions to Stop 3-6**

From Stop 3-5, continue west on dirt road. Note Buick-size clast of megacrystic granite directly north of road after 0.5 miles. Continue another 0.6 miles to west to old water tank and Stop 3-6.

#### **Stop 3-6. Lower Part of Rock Spring Conglomerate**

On the south side of the wash, the conglomerate of Rock Spring interfingers with a thin sequence of basaltic andesite lavas, which have yielded an  $^{40}\text{Ar}/^{39}\text{Ar}$  age of ca. 16.0 Ma. The volcanic component is clearly subordinate to sedimentary rocks in the eastern subbasin of the southern White Hills basin. Exposures here lie in the lower part of the Rock Spring conglomerate, only a few hundred meters east of the nonconformity with Proterozoic basement.

#### **Directions to Stop 3-7**

Continue west on dirt road and keep left (southwest) at Y-intersection 0.4 miles from Stop 3-6. After another 0.2 miles, road veers west and soon passes into Proterozoic gneisses, which directly underlie the Rock Spring conglomerate in this area. Continue west another 1.1 miles, then keep left at Y-intersection.

The road will then cross the approximate trace of the Mountain Spring fault, which is a major west-dipping normal fault that divides the southern White Hills into two discrete subbasins (western volcanic-dominated and eastern sedimentary-dominated subbasins). A narrow northerly trending late Tertiary basin lies in the hanging wall of the Mountain Spring fault in this area, within which the small community of White Hills resides. Displacement on the fault in this area may exceed ~4 km, but decreases appreciably to the south. The Mountain Spring fault can be considered a splay of the Cyclopic–Cerbat Mountains fault system, as it links northward with the Cyclopic fault near Senator Mountain. It may therefore help to accommodate the southward decrease in slip on the South Virgin–White Hills detachment fault.

About 0.9 miles past the Y-intersection, turn right and then immediately left onto wide dirt road. After 0.4 miles, wide road curves 90° to the west into Indian Peak Drive. After traveling

1.0 miles west, turn left onto Senator Boulevard and continue south for 1.2 miles, then veer left onto Skipper Boulevard. Travel 0.4 miles on Skipper Boulevard, then turn right (west) onto paved road of White Hills Boulevard. White Hills Boulevard descends through a small canyon. The surrounding ridges are composed primarily of basaltic andesite lavas tilted  $\sim 25^{\circ}$ – $35^{\circ}$  to the east, which have yielded ca. 16 Ma  $^{40}\text{Ar}/^{39}\text{Ar}$  ages. To the north of the road, gently ( $\sim 10^{\circ}$ ) east-tilted Late Tertiary conglomerate and sandstone onlaps the mafic lavas on the east side of the ridge. From the intersection with Skipper Boulevard, travel west 1.0 miles on White Hills Boulevard to Stop 3-7, where we will take a very short hike to the north of the road.

### Stop 3-7. Early Miocene Nonconformity and Volcanic Rocks

The steeply east-tilted, early Miocene nonconformity (i.e., base of Miocene section) is exposed  $\sim 100$  m north of the road on the lower west flank of the high north-trending ridge. A dacite lava near the base of the section is ca. 18.5 Ma. The dacite-andesite lavas correlate with the volcanics of Dixie Queen Mine, a thick (2–3 km) section of intermediate lavas found in the Mount Perkins area to the west of the Detrital basin (Faulds et al., 1995). Younger, more gently tilted ( $\sim 30^{\circ}$ ), ca. 16 Ma basaltic andesite lavas onlap the steeply tilted ( $\sim 75^{\circ}$ ) volcanics of Dixie Queen Mine on the ridge to the east. The capping mafic lavas to the east are part of a thick synextensional, bimodal volcanic sequence that dominates the western subbasin of the southern White Hills in contrast to the sediment-dominated eastern subbasin.

Beneath the nonconformity to the northwest, extensive mine workings in the Proterozoic gneiss are the remnants of a mining boom in the White Hills more than 100 years ago. The boom town of White Hills was located in this area. The Hualapai and Paiute Indians had long used the iron and manganese oxides associated with veins in the White Hills for paints. This was the Indian Secret mining district, or Silverado district, where gold and silver (“horn silver” or “chloride silver”) was produced from 1892 to 1899 (Huskinson, 1984). Total production was probably 6–8 million ounces of silver and as much as 5000 ounces of gold. In 1899, however, the town of White Hills was destroyed in a flash flood with significant loss of life. The flood still marks one of the worst catastrophes in Arizona history.

### End of Trip, Return to Las Vegas

Continue west on White Hills Road 6.1 miles to U.S. Highway 93. Turn right onto Highway 93 and proceed north to Hoover Dam and Las Vegas.

### SUMMARY

An unusually abrupt boundary separates the Colorado Plateau and Basin and Range province in northwestern Arizona. Little deformed, subhorizontal strata along the western margin of the Colorado Plateau give way westward to moderately to steeply east-tilted fault blocks within the northern Colorado

River extensional corridor across a system of major west-dipping normal faults, which include the Grand Wash and South Virgin–White Hills detachment fault zones. The Grand Wash fault zone forms the main structural and physiographic boundary between the Colorado Plateau and extensional corridor, with as much as 5 km of displacement across some segments. However, the South Virgin–White Hills detachment fault accommodates the greatest amount of extension in the region, having accumulated 5–17 km of normal displacement  $< 30$  km to the west of the plateau margin. Several large basins (east-tilted half grabens) developed in the hanging walls of the Grand Wash and South Virgin–White Hills detachment faults. Foundering of the extensional corridor relative to the Colorado Plateau helped to induce excavation of at least the western part of the Grand Canyon, which was carved into the Colorado Plateau directly east of the corridor.

Cenozoic strata within the hanging walls of the Grand Wash and South Virgin–White Hills detachment faults thus afford an opportunity to assess both the timing of structural demarcation between the Basin and Range and Colorado Plateau and development of the Colorado River. On this trip, we viewed stratigraphic sections and structures in both the hanging wall of the Grand Wash fault (Grand Wash trough and Gregg and Hualapai basins) and hanging wall of the South Virgin–White Hills detachment fault (northern and southern White Hills basins). Tilt fanning within the basins indicates that major east-west extension began ca. 16.5 Ma and had eased significantly by ca. 13 Ma. A northwestward shift of major extension into the western Lake Mead region 13–9 Ma further lowered local base-level in the Basin and Range. However, minor extension continued to at least the early Pliocene and possibly Pleistocene time in some areas, as best evidenced by 300 m of post-6 Ma down-to-the-west displacement on the Wheeler Ridge fault in the Gregg basin (Fig. 8).

These timing constraints indicate that the abrupt boundary between the Colorado Plateau and Basin and Range province in northwest Arizona was taking shape by ca. 16 Ma and had largely developed by ca. 13 Ma. Footwall blocks, including the western margin of the Colorado Plateau, were shedding detritus into the basins as early as ca. 16 Ma. This implies that streams began eroding headward into the Colorado Plateau in the middle Miocene as base level lowered to the west. Excavation of the western Grand Canyon by a small west-flowing stream may have also begun in the middle Miocene. However, thick middle to late Miocene evaporite and lacustrine deposits (e.g., Hualapai Limestone) demonstrate that a long period of internal drainage followed the onset of major extension. The widespread distribution of such deposits and their proximity to the present course of the Colorado River (Fig. 9) may signify a large influx of groundwater and/or surface waters from developing drainage systems, both of which may have been related to subsequent development of the Colorado River. Stratigraphic relations indicate, however, that a through going Colorado River did not arrive in the Lake Mead region until ca. 5.6–4.4 Ma.

## ACKNOWLEDGMENTS

This work was funded by National Science Foundation grants awarded to Faulds (EAR93-16770, EAR99-10977, and EAR-0409913) and Duebendorfer (EAR-9909275 and EAR-0424900), as well as EDMAP cooperative agreements 1434-HQ-96-AG-01546 and 1434-HQ-97-AG-07146) provided by the U.S. Geological Survey (both awarded to Faulds). Duebendorfer gratefully acknowledges support from the donors of the Petroleum Research Fund, administered to the American Chemical Society (PRF 29331-B2). Partial field support was also provided by the U.S. Geological Survey in Las Vegas, Nevada, for which we thank Gary Dixon and Pete Rowley. In addition, the National Park Service at the Lake Mead National Recreation Area has provided critical logistical support for some of this work; special thanks to Kent Turner and Darlene Carnes for this support. Several graduate students have contributed significantly in recent years to our understanding of this region, including Linda Price, Mark Wallace, Nathan Blythe, Brian Coven, Pat Kelleher, and Zack Swaney. In addition, we have benefited greatly from discussions with Sue Beard, Luis Gonzalez, Scott Lundstrom, Dwight Schmidt, Eugene Smith, and Paul Umhoefer. We also thank Terri Garside for help with setting up logistics for the trip and Kris Pizarro for assistance in preparing some of the figures. Constructive reviews by Jon Spencer and Gene Smith improved this manuscript.

## REFERENCES CITED

- Anderson, R.E., 1971, Thin skin distention in Tertiary rocks of southeastern Nevada: *Geological Society of America Bulletin*, v. 82, p. 43–58, doi: 10.1130/0016-7606(1971)82[43:TSDITR]2.0.CO;2.
- Anderson, R.E., 1978, Geologic map of the Black Canyon 15-minute Quadrangle, Mohave county, Arizona and Clark County, Nevada, U.S. Geological Survey Geologic Quadrangle Map GQ-1394, scale 1:62,500.
- Anderson, R.E., and Barnhard, T.P., 1993, Aspects of three-dimensional strain at the margin of the extensional orogen, Virgin River depression area, Nevada, Utah, and Arizona: *Geological Society of America Bulletin*, v. 105, no. 8, p. 1019–1052, doi: 10.1130/0016-7606(1993)105<1019:AOTDSA>2.3.CO;2.
- Anderson, R.E., Longwell, C.R., Armstrong, R.L., and Marvin, R.F., 1972, Significance of K-Ar ages of Tertiary rocks from the Lake Mead region, Nevada-Arizona: *Geological Society of America Bulletin*, v. 83, p. 273–288, doi: 10.1130/0016-7606(1972)83[273:SOKAOT]2.0.CO;2.
- Anderson, R.E., Barnhard, T.P., and Snee, L.W., 1994, Roles of plutonism, mid-crustal flow, tectonic rafting, and horizontal collapse in shaping the Miocene strain field of the Lake Mead area, Nevada and Arizona: *Tectonics*, v. 13, no. 6, p. 1381–1410, doi: 10.1029/94TC01320.
- Beard, L.S., 1996, Paleogeography of the Horse Spring Formation in relation to the Lake Mead fault system, Virgin Mountains, Nevada and Arizona, in Beratan, K.K., ed., *Reconstructing the history of Basin and Range extension using sedimentology and stratigraphy*: Geological Society of America Special Paper 303, p. 27–60.
- Beard, L.S., Anderson, R.E., Block, D.L., Bohannon, R.G., Brady, R.J., Castor, S.B., Duebendorfer, E.M., Faulds, J.E., Felger, T.J., Howard, K.A., Kuntz, M.A., and Williams, V.S., 2007, Preliminary geologic map of the Lake Mead 30' × 60' quadrangle, Clark County, Nevada, and Mohave County, Arizona: U.S. Geological Survey Open-File Report 2007-1010, 109 p., 3 plates, scale 1:100,000 (<http://pubs.usgs.gov/of/2007/1010/>).
- Blacet, P.M., 1975, Preliminary geologic map of the Garnet Mountain quadrangle, Mohave County, Arizona: U.S. Geological Survey Open-File Report 75-93.
- Blackwelder, E., 1934, Origin of the Colorado River: *Geological Society of America Bulletin*, v. 45, p. 551–566.
- Blair, W.N., 1978, Gulf of California in the Lake Mead area of Arizona and Nevada during late Miocene time: *American Association of Petroleum Geologists Bulletin*, v. 62, p. 1159–1170.
- Blair, W.N., and Armstrong, A.K., 1979, Hualapai Limestone Member of the Muddy Creek Formation: The youngest deposit predating the Grand Canyon, southeastern Nevada and northwestern Arizona: U.S. Geological Survey Professional Paper 1111, 14 p.
- Blythe, N.O., 2005, Basin analysis associated with middle-Miocene detachment faulting, eastern Lake Mead region, northwest Arizona [M.S. thesis]: Flagstaff, Northern Arizona University, 225 p.
- Bohannon, R.G., 1984, Nonmarine sedimentary rocks of Tertiary age in the Lake Mead region, southeastern Nevada and northwestern Arizona: U.S. Survey Professional Paper 1259, 72 p.
- Bradbury, J.P., and Blair, W.N., 1979, Paleocology of the upper Miocene Hualapai Limestone Member of the Muddy Creek Formation, northwest Arizona, in Newman, G.W., and Goode, H.D., eds., *Basin and Range symposium and Great Basin field conference*: Rocky Mountain Association of Geologists Guidebook, Denver, p. 292–303.
- Brady, R.J., 1998, The geology of the Gold Butte breakaway zone and the mechanical evolution of normal fault systems [Ph.D. thesis]: California Institute of Technology, Pasadena, 200 p.
- Brady, R., Wernicke, B., and Fryxell, J., 2000, Kinematic evolution of a large-offset continental normal fault system, South Virgin Mountains, Nevada: *Geological Society of America Bulletin*, v. 112, p. 1375–1397, doi: 10.1130/0016-7606(2000)112<1375:KEOALO>2.0.CO;2.
- Brady, R.J., Fryxell, J.E., and Wernicke, B.P., 2008, Geologic map of the Iceberg Canyon Quadrangle, Clark County, Nevada: Nevada Bureau of Mines and Geology Map (in press).
- Buising, A.V., 1990, The Bouse Formation and bracketing units, southeastern California and western Arizona: Implications for the evolution of the proto-Gulf of California and the lower Colorado River: *Journal of Geophysical Research*, v. 95, p. 20,111–20,132.
- Campbell, E.A., and John, B.E., 1996, Constraints on extension-related plutonism from modeling of the Colorado River gravity high: *Geological Society of America Bulletin*, v. 108, no. 10, p. 1242–1255, doi: 10.1130/0016-7606(1996)108<1242:COERPF>2.3.CO;2.
- Cascadden, T.E., 1991, Style of volcanism and extensional tectonics in the eastern Basin and Range Province: Northern Mojave County, Arizona [M.S. thesis]: Las Vegas, University of Nevada, 156 p.
- Castor, S.B., and Faulds, J.E., 2001, Post-6-Ma limestone along the southeast part of the Las Vegas Valley shear zone, southern Nevada, in Young, R.A., and Spamer, E.E., eds., *The Colorado River: Origin and evolution*: Grand Canyon, Arizona, Grand Canyon Association Monograph 12, p. 77–80.
- Castor, S.B., Faulds, J.E., Rowland, S.M., and dePolo, C.M., 2000, Geologic map of the Frenchman Mountain Quadrangle, Clark County, Nevada: Nevada Bureau of Mines and Geology Map 127, with accompanying text, scale 1:24,000.
- Crossey, L.J., Karlstrom, L.E., Patchett, P.J., Hilton, D., Fischer, T., Sharp, W., Pederson, J., Schmidt, D.L., Antweiler, R.C., and Reynolds, A.C., 2002, Active springs and Quaternary travertines in Grand Canyon; Linking modern and paleo-hydrologic systems: *Geological Society of America Abstracts with Programs*, v. 34, no. 6, paper No. 175–16.
- Davis, G.A., and Lister, G.S., 1988, Detachment faulting in continental extension: Perspectives from the southwestern U.S. Cordillera, in Clark, S.P., Burchfiel, B.C., and Suppe, J. eds., *Processes in Continental Lithospheric Deformation*: Geological Society of America Special Paper 218, p. 133–159.
- Davis, G.A., Anderson, J.L., Frost, E.G., and Shackelford, T.J., 1980, Mylonitization and detachment faulting in the Whipple-Buckskin-Rawhide Mountains terrane, southeastern California and western Arizona, in Crittenden, M.D., Coney, P.J., and Davis, G.H., eds., *Cordilleran metamorphic core complexes*: Geological Society of America Memoir 153, p. 79–130.
- Dorsey, R.J., Fluette, A., McDougall, K., Housen, B.A., and Janecke, S.U., 2005, Terminal Miocene arrival of Colorado River sand in the Salton Trough, southern California: Implication for initiation of the lower Colorado River drainage: *Geological Society of America Abstracts with Programs*, v. 37, no. 7, p. 109.
- Dorsey, R.J., Fluette, A., McDougall, K., Housen, B.A., Janecke, S.U., Axen, G.J., and Shirvell, C.R., 2007, Chronology of Miocene–Pliocene deposits at Split Mountain Gorge, Southern California: A record of regional tectonics and Colorado River evolution: *Geology*, v. 35, p. 57–60, doi: 10.1130/G23139A.1

- Duebendorfer, E.M., and Sharp, W.D., 1998, Variation in displacement along strike of the South Virgin–White Hills detachment fault: Perspective from the northern White Hills, northwestern Arizona: *Geological Society of America Bulletin*, v. 110, p. 1574–1589, doi: 10.1130/0016-7606(1998)110<1574:VIDASO>2.3.CO;2.
- Duebendorfer, E.M., and Simpson, D.A., 1994, Kinematics and timing of Tertiary extension in the western Lake Mead region, Nevada: *Geological Society of America Bulletin*, v. 106, no. 8, p. 1057–1073, doi: 10.1130/0016-7606(1994)106<1057:KATOTE>2.3.CO;2.
- Duebendorfer, E.M., and Wallin, E.T., 1991, Basin development and syntectonic sedimentation associated with kinematically coupled strike-slip and detachment faulting, southern Nevada: *Geology*, v. 19, p. 87–90, doi: 10.1130/0091-7613(1991)019<0087:BDASSA>2.3.CO;2.
- Duebendorfer, E.M., Chamberlain, K.R., and Jones, C.S., 2001, Paleoproterozoic tectonic history of the Mojave–Yavapai boundary zone: Perspective from the Cerbat Mountains, northwestern Arizona: *Geological Society of America Bulletin*, v. 113, p. 575–590, doi: 10.1130/0016-7606(2001)113<0575:PTHOTC>2.0.CO;2.
- Faulds, J.E., 1996, Geologic map of the Fire Mountain Quadrangle, Clark County, Nevada, and Mohave County, Arizona: Nevada Bureau of Mines and Geology Map 106, scale 1:24,000 (with accompanying text).
- Faulds, J.E., 1999, Cenozoic geology of the northern Colorado River extensional corridor, southern Nevada and northwest Arizona: Road logs and discussion: Nevada Petroleum Society Guidebook, p. 1–96.
- Faulds, J.E., and Varga, R.J., 1998, The role of accommodation zones and transfer zones in the regional segmentation of extended terranes, *in* Faulds, J.E., and Stewart, J.H., eds., *Accommodation Zones and Transfer Zones: The Regional Segmentation of the Basin and Range Province*: Geological Society of America Special Paper 323, p. 1–46.
- Faulds, J.E., Geissman, J.W., and Mawer, C.K., 1990, Structural development of a major accommodation zone in the Basin and Range province, northwestern Arizona and southern Nevada, *in* Wernicke, B., ed., *Basin and Range extensional tectonics near the latitude of Las Vegas, Nevada*: Geological Society of America Memoir 176, p. 37–76.
- Faulds, J.E., Feuerbach, D.L., Reagan, M.K., Metcalf, R.V., Gans, P., and Walker, J.D., 1995, The Mt. Perkins block, northwestern Arizona: An exposed cross section of an evolving, preextensional to synextensional magmatic system: *Journal of Geophysical Research*, v. 100, no. B8, p. 15,249–15,266, doi: 10.1029/95JB01375.
- Faulds, J.E., Schreiber, B.C., Reynolds, S.J., Gonzalez, L., and Okaya, D., 1997, Origin and paleogeography of an immense, nonmarine Miocene salt deposit in the Basin and Range (western USA): *The Journal of Geology*, v. 105, p. 19–36.
- Faulds, J.E., Smith, E.I., and Gans, P.B., 1999, Spatial and temporal patterns of magmatism and extension in the northern Colorado River extensional corridor, Nevada and Arizona: A preliminary report: Nevada Petroleum Society Guidebook, p. 171–183.
- Faulds, J.E., Feuerbach, D.L., Miller, C.F., and Smith, E.I., 2001a, Cenozoic evolution of the northern Colorado River extensional corridor, southern Nevada and northwest Arizona: Pacific Section of the American Association of Petroleum Geologists Publication GB 78 (also Utah Geological Association Publication 30), p. 239–272.
- Faulds, J.E., Price, L.M., and Wallace, M.A., 2001b, Pre-Colorado river paleogeography and extension along the Colorado Plateau–Basin and Range boundary, northwest Arizona, *in* Young, R.A., and Spamer, E.E., eds., *The Colorado River: Origin and evolution*: Grand Canyon, Arizona, Grand Canyon Association Monograph 12, p. 93–99.
- Faulds, J.E., Wallace, M.A., Gonzalez, L.A., and Heizler, M., 2001c, Depositional environment and paleogeographic implications of the late Miocene Hualapai Limestone, northwest Arizona and southern Nevada, *in* Young, R.A., and Spamer, E.E., eds., *The Colorado River: Origin and evolution*: Grand Canyon, Arizona, Grand Canyon Association Monograph 12, p. 81–87.
- Faulds, J.E., Gonzalez, L.A., Perkins, M.E., House, P.K., Pearthree, P.A., Castor, S.B., and Patchett, P.J., 2002a, Late Miocene–early Pliocene transition from lacustrine to fluvial deposition: Inception of the lower Colorado River in southern Nevada and northwest Arizona: *Geological Society of America Abstracts with Programs*, v. 34, no. 4, p. 60.
- Faulds, J.E., Olson, E.L., Harlan, S.S., and McIntosh, W.C., 2002b, Miocene extension and fault-related folding in the Highland Range, southern Nevada: A three-dimensional perspective: *Journal of Structural Geology*, v. 24, p. 861–886, doi: 10.1016/S0191-8141(01)00116-X.
- Fenton, C.R., Webb, R.H., Pearthree, P.A., Cerling, T.E., and Poreda, R.J., 2001, Displacement rates on the Toroweap and Hurricane faults: Implications for Quaternary downcutting in the Grand Canyon, Arizona: *Geology*, v. 29, no. 11, p. 1035–1038, doi: 10.1130/0091-7613(2001)029<1035:DROTTA>2.0.CO;2.
- F.E.R.C., 1982, Red Lake salt cavern, gas storage project; final environmental impact statement: Federal Energy Regulatory Commission, Office of Pipeline and Producer Regulation, EIS-0028, 217 p.
- Feuerbach, D.L., Smith, E.I., Tangeman, J.A., and Walker, J.D., 1993, The role of the mantle during crustal extension: Constraints from geochemistry of volcanic rocks in the Lake Mead area, Nevada and Arizona: *Geological Society of America Bulletin*, v. 105, p. 1561–1575, doi: 10.1130/0016-7606(1993)105<1561:TROTMD>2.3.CO;2.
- Fitzgerald, P.G., Fryxell, J.E., and Wernicke, B.P., 1991, Apatite fission track constraints on the extensional evolution of the Gold Butte crustal section, South Virgin Mountains, Nevada: *Geology*, v. 19, p. 1013–1016, doi: 10.1130/0091-7613(1991)019<1013:MCEAU>2.3.CO;2.
- Fitzgerald, P.G., O’Sullivan, P.B., Duebendorfer, E.M., Faulds, J.E., and Fryxell, J.E., 2003, Thermochronologic constraints on extension via detachment faulting in the White Hills of northwest Arizona and Gold Butte Block of southeast Nevada: *Geological Society of America Abstracts with Programs*, v. 35, no. 6, p. 348.
- Fryxell, J.E., Salton, C.G., Selverstone, J., and Wernicke, B., 1992, Gold Butte crustal section, South Virgin Mountains, Nevada: *Tectonics*, v. 11, p. 1099–1120.
- Gans, P.B., and Bohron, W.A., 1998, Suppression of volcanism during rapid extension in the Basin and Range province, United States: *Science*, v. 279, p. 66–68, doi: 10.1126/science.279.5347.66.
- Gans, P.B., Mahood, G.A., and Schermer, E., 1989, Synextensional magmatism in the Basin and Range province: A case study in the eastern Great Basin: *Geological Society of America Special Paper* 233, 53 p.
- Glazner, A.F., and Bartley, J.M., 1984, Timing and tectonic setting of Tertiary low-angle normal faulting and associated magmatism in the southwestern United States: *Tectonics*, v. 3, p. 85–96.
- Glazner, A.F., Nielson, J.E., Howard, K.A., and Miller, D.M., 1986, Correlation of the Peach Spring Tuff, a large-volume Miocene ignimbrite sheet in California and Arizona: *Geology*, v. 14, p. 840–843, doi: 10.1130/0091-7613(1986)14<840:COTPST>2.0.CO;2.
- Goetz, A.F.H., Billingsley, F.C., Gillespie, A.R., Abrams, M.J., Squires, R.L., Shoemaker, E.M., Lucchitta, I., and Elston, D.P., 1975, Application of ERTS images and image processing to regional geologic problems and geologic mapping in northern Arizona: Jet Propulsion Laboratory Technical Report 32-1597, 188 p.
- Harlan, S.S., Duebendorfer, E.M., and Deibert, J.E., 1998, <sup>40</sup>Ar/<sup>39</sup>Ar age determinations from Miocene volcanic rocks in the western Lake Mead area and southern Las Vegas Range, Nevada: *Canadian Journal of Earth Sciences*, v. 35, p. 495–503, doi: 10.1139/cjes-35-5-495.
- Heckel, P.H., 1972, Recognition of ancient shallow marine environments, *in* Rigby, J.K., and Hamblin, W.K., eds., *Recognition of ancient sedimentary environments*, Society of Economic Paleontologists and Mineralogists Special Publication, v. 16, p. 226–286.
- Hillhouse, J.W., and Wells, R.E., 1991, Magnetic fabric, flow directions, and source area of the lower Miocene Peach Springs Tuff in Arizona, California, and Nevada: *Journal of Geophysical Research*, v. 96, no. B7, p. 12,443–12,460.
- House, P.K., Pearthree, P.A., Howard, K.A., Bell, J.W., Perkins, M.E., Faulds, J.E., and Brock, A.L., 2005, Birth of the lower Colorado River—Stratigraphic and geomorphic evidence for its inception near the conjunction of Nevada, Arizona, and California, *in* Pederson, J., and Dehler, C.M., eds., *Interior western United States*: Geological Society of America Field Guide 6, p. 357–387, doi:10.1130/2005.fld006(17).
- Howard, K.A., and Bohannon, R.G., 2001, Lower Colorado River; Framework, Neogene deposits, incision, and evolution, *in* Young, R.A., and Spamer, E.E., eds., *The Colorado River: Origin and evolution*: Grand Canyon, Arizona, Grand Canyon Association Monograph 12, p. 101–105.
- Howard, K.A., and John, B.E., 1987, Crustal extension along a rooted system of imbricate low-angle faults: Colorado River extensional corridor, California and Arizona, *in* Coward, M.P., Dewey, J.F., and Hancock, P.L., eds., *Continental Extensional Tectonics*: Geological Society of London Special Publication 28, p. 299–311.
- Howard, K.A., Faulds, J.E., Beard, L.S., and Kunk, M.J., 2000, Reverse-drag folding across the path of the antecedent early Pliocene Colorado River below the mouth of the Grand Canyon: Implications for plateau uplift: *Geological Society of America Abstracts with Programs*, v. 32, no. 7, p. 41.

- Howard, K.A., Hook, S.J., Phelps, G.A., and Block, D.L., 2003, Geologic map of the Hiller Mountains Quadrangle, Clark County, Nevada and Mohave County, Arizona: Nevada Bureau of Mines and Geology Map 137, scale 1:24,000, 8 p.
- Howard, K.A., Lundstrom, S.C., Malmon, D.V., and Hooke, S.J., 2008, Age, distribution, and formation of late Cenozoic paleovalleys of the lower Colorado River and their relation to river aggradation and degradation, *in* Reheis, M.C., Herschler, R., and Miller, D.M., eds., Late Cenozoic Drainage History of the Southwestern Great Basin and Lower Colorado River Region: Geologic and Biotic Perspectives: Geological Society of America Special Paper 439, doi: 10.1130/2008.2439(18) (in press).
- Hunt, C.B., 1969, Geologic history of the Colorado River, *in* The Colorado River region and John Wesley Powell: U.S. Geological Survey Professional Paper 600-B, p. B169–B177.
- Huntoon, P.W., 1996, Large-basin ground water circulation and paleo-reconstruction of circulation leading to uranium mineralization in Grand Canyon breccia pipes, Arizona: *Mountain Geologist*, v. 33, p. 71–84.
- Huntoon, P.W., 2000, Variability of karstic permeability between unconfined and confined aquifers, Grand Canyon region, Arizona: *Environmental & Engineering Geoscience*, v. 6, p. 155–170.
- Huskinson, E., Jr., 1984, The White Hills Mines, Indian Secret mining district, Mohave County, Arizona: *Arizona Geological Society Fall Field Trip*, 5 p.
- Larsen, L.L., and Smith, E.I., 1990, Mafic enclaves in the Wilson Ridge pluton, northwestern Arizona: Implications for the generation of a calc-alkaline pluton in an extensional environment: *Journal of Geophysical Research*, v. 95, p. 17,693–17,716.
- Longwell, C.R., 1928, Geology of the Muddy Mountains, Nevada: U.S. Geological Survey Bulletin 798, 152 p.
- Longwell, C.R., 1936, Geology of the Boulder Reservoir floor, Arizona-Nevada: *Geological Society of America Bulletin*, v. 47, p. 1393–1476.
- Longwell, C.R., 1946, How old is the Colorado River: *American Journal of Science*, v. 244, p. 817–835.
- Longwell, C.R., 1974, Measure and date of movement on Las Vegas Valley shear zone, Clark County, Nevada: *Geological Society of America Bulletin*, v. 85, p. 985–990, doi: 10.1130/0016-7606(1974)85<985:MADOMO>2.0.CO;2.
- Lucchitta, I., 1966, Cenozoic geology of the upper Lake Mead area adjacent to the Grand Wash cliffs, Arizona [Ph.D. thesis]: University Park, Pennsylvania State University, 218 p.
- Lucchitta, I., 1972, Early history of the Colorado River in the Basin and Range province: *Geological Society of America Bulletin*, v. 83, p. 1933–1948, doi: 10.1130/0016-7606(1972)83[1933:EHOTCR]2.0.CO;2.
- Lucchitta, I., 1979, Late Cenozoic uplift of the southwestern Colorado Plateau and adjacent lower Colorado River region: *Tectonophysics*, v. 61, p. 63–95, doi: 10.1016/0040-1951(79)90292-0.
- Lucchitta, I., 1989, History of the Grand Canyon and of the Colorado River in Arizona: *Arizona Geological Society Digest*, v. 17, p. 701–715.
- Lucchitta, I., 1998, The upper Miocene Bouse Formation as an indicator for late Cenozoic uplift of the Colorado Plateau: *Geological Society of America Abstracts with Programs*, v. 30, no. 6, p. 14.
- Lucchitta, I., and Young, R.A., 1986, Structure and geomorphic character of western Colorado Plateau in the Grand Canyon-Lake Mead region, *in* Nations, J.D., Conway, C.M., and Swann, G.A., eds., *Geology of central and northern Arizona: Geological Society of America Rocky Mountain Section Guidebook*, Flagstaff, Northern Arizona University, p. 159–176.
- Lucchitta, I., Beard, L.S., and Rieck, H.J., 1986, Geologic map of the Pigeon Canyon, Nevershine Mesa, and Snap Point Wilderness Study Areas, Mohave County, Arizona: U.S. Geological Survey Miscellaneous Field Studies Map 1860-B, scale 1:50,000.
- Mannion, L.E., 1963, Virgin River salt deposits, Clark County, Nevada, *in* Bersticker, A.C., Hoekstra, K.E., and Hall, J.F., eds., *Symposium on salt: Northern Ohio Geological Society*, v. 1, p. 166–175.
- McCarthy, J., Larkin, S.P., Fuis, G.S., Howard, K.A., and Simpson, R.W., 1991, Anatomy of a metamorphic core complex: Seismic refraction/wide-angle reflection profiling in southeastern California and western Arizona: *Journal of Geophysical Research*, v. 96, p. 12,259–12,291.
- McKee, E.D., and McKee, E.H., 1972, Pliocene uplift of the Grand Canyon region: Time of drainage adjustment: *Geological Society of America Bulletin*, v. 83, p. 1923–1932, doi: 10.1130/0016-7606(1972)83[1923:PUOTGC]2.0.CO;2.
- Metzger, D.G., 1968, The Bouse Formation (Pliocene) of the Parker-Blythe-Cibola area, Arizona and California: U.S. Geological Survey Professional Paper 600-D, p. 126–136.
- Mills, J.G., 1994, Geologic map of the Hoover Dam Quadrangle: Nevada Bureau of Mines and Geology Map 102, 1:24,000 scale.
- Morikawa, S.A., 1994, The geology of the tuff of Bridge Spring, southern Nevada and northwestern Arizona [M.S. thesis]: Las Vegas, University of Nevada, 165 p.
- Myers, I.A., Smith, E.I., and Wyman, R.V., 1986, Control of gold mineralization at the Cyclopic Mine, Gold Basin District, Mojave County, Arizona: *Economic Geology and the Bulletin of the Society of Economic Geologists*, v. 81, p. 1553–1557.
- Nations, J., 1989, Cretaceous history of northeastern and east-central Arizona, *in* Jenney, J.P., and Reynolds, S.J., eds., *Geologic evolution of Arizona: Arizona Geological Society Digest*, v. 17, p. 435–446.
- Nielson, J.E., Lux, D.R., Dalrymple, G.B., and Glazner, A.F., 1990, Age of the Peach Springs Tuff, southeastern California and western Arizona: *Journal of Geophysical Research*, v. 95, p. 571–580.
- Parsons, T., and McCarthy, J., 1995, The active southwest margin of the Colorado Plateau: Uplift of mantle origin: *Geological Society of America Bulletin*, v. 107, no. 2, p. 139–147, doi: 10.1130/0016-7606(1995)107<0139:TASMOT>2.3.CO;2.
- Pederson, J.L., and Karlstrom, K.E., 2001, Relating differential incision of Grand Canyon to slip along the Hurricane/Toroweap fault system, *in* Young, R.A., and Spamer, E.E., eds., *The Colorado River: Origin and evolution: Grand Canyon, Arizona*, Grand Canyon Association Monograph 12, p. 159–165.
- Pederson, J., Karlstrom, K., Sharp, W., and McIntosh, W., 2002, Differential incision of the Grand Canyon related to Quaternary faulting—Constraints from U-series and Ar/Ar dating: *Geology*, v. 30, no. 8, p. 739–742, doi: 10.1130/0091-7613(2002)030<0739:DIOTGC>2.0.CO;2.
- Peirce, H.W., 1976, Tectonic significance of Basin and Range thick evaporite deposits: *Arizona Geological Society Digest*, v. 10, p. 325–339.
- Peirce, H.W., 1985, Arizona's backbone: the transition zone, Arizona Bureau of Geology and Mineral Technology: *Fieldnotes*, v. 15, p. 1–6.
- Powell, J.W., 1875, *Exploration of the Colorado River of the West and its tributaries: Explored in 1869, 1870, 1871, and 1872: Washington, D.C., U.S. Government Printing Office*, 291 p.
- Powell, J.E., 1895, *Canyons of the Colorado River: Meadville, Pennsylvania, Flood and Vincent, The Chautauqua-Century Press*, 400 p.
- Price, L.M., 1997, Geometry and evolution of a major segment of the Grand Wash fault zone, southern White Hills, northwestern Arizona [M.S. thesis]: University of Iowa, Iowa City, 147 p.
- Price, L.M., and Faulds, J.E., 1999, Structural development of a major segment of the Colorado Plateau-Basin and Range boundary, southern White Hills, Arizona: *Nevada Petroleum Society Guidebook*, p. 139–170.
- Reiners, P.W., 2002, (U-Th)/He chronometry experiences a renaissance: *Eos (Transactions, American Geophysical Union)*, v. 83, no. 3, p. 21–27.
- Reiners, P.W., Brady, R., Farley, K.A., Fryxell, J.E., Wernicke, B., and Lux, D., 2000, Helium and argon thermochronometry of the Gold Butte block, South Virgin Mountains, Nevada: *Earth and Planetary Science Letters*, v. 178, p. 315–326.
- Roskowski, J.A., Patchett, P.J., Pearthree, P.A., Spencer, J.E., Faulds, J.E., and Reynolds, A.C., 2007, A late Miocene-early Pliocene chain of lakes fed by the Colorado River: Evidence from Sr isotopes of the Bouse Formation between Grand Canyon and Gulf of California: *Geological Society of America Abstracts with Programs*, v. 39, no. 6, p. 435.
- Sherrod, D., and Nielson, J., eds., 1993, *Tertiary stratigraphy of highly extended terranes, California, Arizona, and Nevada: U.S. Geological Survey Bulletin 2053*.
- Silver, L.T., Bickford, M.E., Van, S.W.R., Anderson, J.L., Anderson, T.H., and Madaris, L.G., 1977, The 1.4–1.5 b.y. transcontinental anorogenic plutonic perforation of North America: *Geological Society of America Abstracts with Programs*, v. 9, no. 7, p. 1176–1177.
- Smith, P.B., 1970, New evidence for a Pliocene marine embayment along the lower Colorado River area, California and Arizona: *Geological Society of America Bulletin*, v. 81, p. 1411–1420, doi: 10.1130/0016-7606(1970)81[1411:NEFAPM]2.0.CO;2.
- Spencer, J.E., and Patchett, P.J., 1997, Sr isotope evidence for a lacustrine origin for the upper Miocene to Pliocene Bouse Formation, lower Colorado River trough, and implications for timing of Colorado Plateau uplift: *Geological Society of America Bulletin*, v. 109, p. 767–778, doi: 10.1130/0016-7606(1997)109<0767:SIEFAL>2.3.CO;2.
- Spencer, J.E., and Pearthree, P.A., 2001, Headward erosion versus closed-basin spillover as alternative causes of Neogene capture of the ancestral Colo-

- rado River by the Gulf of California, *in* Young, R.A., and Spamer, E.E., eds., *The Colorado River: Origin and evolution: Grand Canyon, Arizona*, Grand Canyon Association Monograph 12, p. 215–219.
- Spencer, J.E., and Reynolds, S.J., 1989, Middle Tertiary tectonics of Arizona and adjacent areas, *in* Jenney, J.P. and Reynolds, S.J., eds., *Geologic evolution of Arizona: Arizona Geological Society Digest 17*, p. 539–574.
- Spencer, J.E., Peters, L., McIntosh, W.C., and Patchett, P.J., 2001,  $^{40}\text{Ar}/^{39}\text{Ar}$  geochronology of the Hualapai Limestone and Bouse Formation and implications for the age of the lower Colorado River, *in* Young, R.A., and Spamer, E.E., eds., *The Colorado River: Origin and evolution: Grand Canyon, Arizona*, Grand Canyon Association Monograph 12, p.89–92.
- Swaney, Z.A., 2005, Tilting history of the Lost Basin Range and western Grand Wash trough, northwest Arizona: Regional implications [M.S. thesis]: Northern Arizona University, Flagstaff, 144 p.
- Talbot, M.R., and Kelts, K., 1990, Paleolimnological signatures from carbon and oxygen isotopic ratios in carbonates from organic carbon-rich lacustrine sediments, *in* Katz, B.J., ed., *Lacustrine Basin Exploration: Case Studies and Modern Analogs: American Association of Petroleum Geologists Memoir 50*, p. 99–112.
- Topping, D.J., 1993, Paleogeographic reconstruction of the Death Valley extended region: Evidence from Miocene large rock-avalanche deposits in the Amargosa Chaos Basin, California: *Geological Society of America Bulletin*, v. 105, p. 1190–1213, doi: 10.1130/0016-7606(1993)105<1190:PROTDV>2.3.CO;2.
- Varga, R.J., Faulds, J.E., Snee, L.W., Harlan, S.S., and Bettison-Varga, L., 2004, Miocene extension and extensional folding in an anticlinal segment of the Black Mountains accommodation zone, Colorado River extensional corridor, southwestern USA: *Tectonics*, v. 23, no. 11, TC109, doi: 10.1029/2002TC001454], 19 p.
- Volborth, A., 1962, Rapakivi-type granites in the Precambrian complex of Gold Butte, Clark County, Nevada: *Geological Society of America Bulletin*, v. 73, no. 7, p. 813–831, doi: 10.1130/0016-7606(1962)73[813:RGITPC]2.0.CO;2.
- Wallace, M.A., 1999, Cenozoic stratigraphic and structural framework of the southern Grand Wash trough, northwestern Arizona: Paleogeographic implications [M.S. thesis]: University of Iowa, Iowa City, 119 p.
- Wallace, M.W., Faulds, J.E., and Brady, R.J., 2005, Geologic map of the Meadview North Quadrangle, Arizona and Nevada: Nevada Bureau of Mines and Geology Map, scale 1:24,000, 22 p. text.
- Weber, M.E., and Smith, E.I., 1987, Structural and geochemical constraints on the reassembly of mid-Tertiary volcanoes in the Lake Mead area of southern Nevada: *Geology*, v. 15, p. 553–556, doi: 10.1130/0091-7613(1987)15<553:SAGCOT>2.0.CO;2.
- Wenrich, K.J., Billingsley, G.H., and Huntoon, P.W., 1996, Breccia-pipe and geologic map of the northwestern part of the Hualapai Indian Reservation and vicinity, Arizona: U.S. Geological Survey Geologic Investigations Map I-2522, scale 1:48,000.
- Wernicke, B., and Axen, G.J., 1988, On the role of isostasy in the evolution of normal fault systems: *Geology*, v. 16, p. 848–851, doi: 10.1130/0091-7613(1988)016<0848:OTROII>2.3.CO;2.
- Yarnold, J.C., and Lombard, J.P., 1989, A facies model for large rock-avalanche deposits formed in dry climates, *in* Colburn, I.P., Abbott, P.L., and Minch, J., eds., *Conglomerates in basin analysis: A symposium dedicated to A.O. Woodward: Pacific Section of Society of Economic Paleontologists and Mineralogists*, v. 62, p. 9–31.
- Young, R.A., 1982, Paleogeomorphic evidence for the structural history of the Colorado Plateau margin in western Arizona, *in* Frost, E.G., and Martin, D.M., eds., *Mesozoic-Cenozoic tectonic evolution of the Colorado River region, California, Arizona, and Nevada: Cordilleran Publishers, San Diego*, 608 p.
- Young, R.A., and Brennan, W.J., 1974, Peach Springs Tuff; Its bearing on structural evolution of the Colorado Plateau and development of Cenozoic drainage in Mohave County, Arizona: *Geological Society of America Bulletin*, v. 85, p. 83–90, doi: 10.1130/0016-7606(1974)85<83: PSTIBO>2.0.CO;2.
- Young, R.A., and Spamer, E.E., eds., 2001, *The Colorado River: Origin and evolution: Grand Canyon, Arizona: Grand Canyon Association Monograph 12*, 280 p.